

71093

GAMMA-RAY SPECTROSCOPY OF EXCITED STATES

IN  $^{177}\text{Hf}$  AND  $^{182}\text{W}$

by

Brian Douglas Jeltema

NOTICE

This report was prepared as an account of work sponsored by the United States Government. Neither the United States nor the United States Atomic Energy Commission, nor any of their employees, nor any of their contractors, subcontractors, or their employees, makes any warranty, express or implied, or assumes any legal liability or responsibility for the accuracy, completeness or usefulness of any information, apparatus, product or process disclosed, or represents that its use would not infringe privately owned rights.

A DISSERTATION

Submitted to

Michigan State University

in partial fulfillment of the requirements

for the degree of

MASTER OF SCIENCE

Department of Chemistry

1974

DISTRIBUTION OF THIS DOCUMENT UNLIMITED

feg

## **DISCLAIMER**

**This report was prepared as an account of work sponsored by an agency of the United States Government. Neither the United States Government nor any agency Thereof, nor any of their employees, makes any warranty, express or implied, or assumes any legal liability or responsibility for the accuracy, completeness, or usefulness of any information, apparatus, product, or process disclosed, or represents that its use would not infringe privately owned rights. Reference herein to any specific commercial product, process, or service by trade name, trademark, manufacturer, or otherwise does not necessarily constitute or imply its endorsement, recommendation, or favoring by the United States Government or any agency thereof. The views and opinions of authors expressed herein do not necessarily state or reflect those of the United States Government or any agency thereof.**

## **DISCLAIMER**

**Portions of this document may be illegible in electronic image products. Images are produced from the best available original document.**

ABSTRACT

GAMMA-RAY SPECTROSCOPY OF EXCITED STATES  
IN  $^{177}\text{Hf}$  AND  $^{182}\text{W}$

by

Brian Douglas Jeltema

The deformed nuclei  $^{177}\text{Hf}$  and  $^{182}\text{W}$  were investigated via  $\gamma$ -ray spectroscopic techniques. The EC- $\beta^+$  decay of  $^{177}\text{Ta}$  to  $^{177}\text{Hf}$  was investigated in  $\gamma$ -ray singles and  $\gamma$ - $\gamma$  coincidence spectroscopy. Thirteen energy levels in  $^{177}\text{Hf}$  were deduced; four levels and fourteen  $\gamma$  rays associated with  $^{177}\text{Ta}$  decay were unknown from previous NaI(Tl) work. Logft values have been assigned to the decay, and multipolarities of several transitions have been assigned with use of earlier conversion electron data.

The  $^{182}\text{W}$  level scheme was investigated primarily by in-beam  $\gamma$ -ray spectroscopy. A total of 59 excited states were placed by use of three-parameter ( $\gamma$ - $\gamma$ -t) coincidence data. Eleven rotational bands were deduced in this investigation and all were given collective or particle assignments. The ground state rotational band was seen at least to spin 12, and the rotational band based on a 1.4  $\mu\text{s}$  isomer was established to spin 15. Decay patterns of some bands are explained qualitatively in terms of configuration mixing, and  $\beta^-$ ,  $\gamma^-$ , ground-band mixing calculations were carried out in an attempt to explain the apparent perturbations present in those three bands.

The in-beam study of  $^{182}\text{W}$  indicated that errors exist in the accepted decay scheme for 64 h  $^{182m}\text{Re}$ . Therefore a brief study of this decay was also carried out. Two-parameter  $\gamma$ - $\gamma$  coincidence data were collected, and  $\gamma$ -ray intensities in the region from 84 keV to 360 keV were measured. A level scheme consistent with the decay and in-beam  $\gamma$ -ray data was established, and  $\log ft$  values were assigned.

GAMMA-RAY SPECTROSCOPY OF EXCITED STATES  
IN  $^{177}\text{Hf}$  AND  $^{182}\text{W}$

by

Brian Douglas Jeltema

A DISSERTATION  
Submitted to  
Michigan State University  
in partial fulfillment of the requirements  
for the degree of

MASTER OF SCIENCE

Department of Chemistry

1974

#### ACKNOWLEDGEMENTS

I wish to thank Dr. H. G. Blosser, Dr. P. Miller, and the staff of the MSU Cyclotron for making the experimental work possible, as well as Mr. R. Au and the computer staff for their aid in data accumulation and evaluation.

The assistance and advice of Dr. Wm. C. McHarris and Dr. W. H. Kelly has been very helpful and is greatly appreciated.

Dr. R. A. Warner and Dr. T. L. Khoo have provided many helpful discussions during my stay at MSU, and in addition have been invaluable during the experimental portions of this project.

The other members of our research group deserve special thanks both for assistance and for warm friendship extended during our acquaintance.

I wish to thank Dr. G. Sletten for furnishing some of the targets used in these experiments, and Ms. Lee Creswell for typing much of the manuscript.

Finally, I especially wish to thank Dr. F. M. Bernthal for suggesting this field of study, and for his interest, support, and friendship of the last two years.

I acknowledge the financial assistance of the National Science Foundation, the Atomic Energy Commission, and Michigan State University.

TABLE OF CONTENTS

	PAGE
ACKNOWLEDGEMENTS .. . . . .	ii
LIST OF TABLES .. . . . .	iv
LIST OF FIGURES .. . . . .	v
I. INTRODUCTION .. . . . .	1
II. THE DECAY OF $^{177}\text{Ta}$ TO $^{177}\text{Hf}$ .. . . . .	3
A. Introduction .. . . . .	3
B. Experimental and Discussion .. . . . .	4
III. THE IN BEAM $\gamma$ -RAY STUDY OF $^{182}\text{W}$ .. . . . .	13
A. Introduction .. . . . .	13
B. Experimental .. . . . .	14
C. Experimental Results .. . . . .	16
D. Construction of the Level Scheme .. . . . .	24
1. Even Parity Bands .. . . . .	36
2. Odd Parity Bands .. . . . .	65
E. Summary and Conclusions .. . . . .	72
IV. THE DECAY OF $^{182m}\text{Re}$ TO $^{182}\text{W}$ .. . . . .	74
BIBLIOGRAPHY .. . . . .	83

LIST OF TABLES

TABLE	PAGE
1 Results of Coriolis-Mixing Energy Fit for Even-Parity States in $^{177}\text{Hf}$ .. .. ..	8
2 Characteristics of Detectors Used in Study of $^{182}\text{W}$ .. .. .. .. .. ..	15
3 $\gamma$ -Rays Observed Following the $^{180}\text{Hf}(\alpha, 2n)^{182}\text{W}$ Reaction at 26 MeV .. .. .. ..	19
4 Parameters Obtained in Three Band Mixing Calculations .. .. .. .. ..	49
5 Results of 3-Band-Mixing Fits .. ..	50
6 $g_K$ from Branching Ratios for $^{182}\text{W}$ Bands ..	56
7 Comparison of Experimental $B(E2)$ Ratios with Alagas Rules for the $\gamma$ and $K^T = 6^+$ Bands ..	60
8 $\gamma$ -Rays Associated with the Decay of $^{182m}\text{Re}$	76

LIST OF FIGURES

FIGURE	PAGE
1 The $\gamma$ -ray singles spectrum of $^{177}\text{Ta}$ . A Cd-Cu absorber was used to attenuate the intense x-rays and 113-keV transition .....	5
2 The $^{177}\text{Ta}$ decay scheme. All transitions are placed on the basis of coincidence data except those associated with the 873.0-keV level .....	6
3 The in-beam $\gamma$ -ray singles spectrum resulting from the $^{180}\text{Hf}(\alpha, 2n)^{182}\text{W}$ reaction .....	17
4 The high-resolution in-beam $\gamma$ -ray singles spectrum resulting from the $^{180}\text{Hf}(\alpha, 2n)^{182}\text{W}$ reaction .....	18
5 The integral coincidence spectra obtained for $^{182}\text{W}$ ..	25
6 Coincidence gates associated with the $K^\pi = 2^-$ octupole band .....	26
7 Coincidence gates associated with the $K^\pi = 2^-$ octupole band (Contd.) .....	27
8 Coincidence gates associated with the $K^\pi = 6^+$ band ..	28
9 Coincidence gates associated with the $K^\pi = 7^-$ band ..	29
10 Coincidence gates associated with the $K^\pi = 8^-$ band ..	
11 A partial level scheme for states ranging from ground to 2230.6 keV in $^{182}\text{W}$ . All known transitions are shown. Dots are below those transitions placed on the basis of coincidence data obtained in this study. Asterisks (*) behind $\gamma$ -ray energies indicates that the transition is known only from decay studies [Ha61, Sa70, Ga72]. The level at 1137 keV is taken from Kleinheinz <i>et al.</i> [K173]. ..	32
12 A partial level scheme for states ranging from 1487.5 keV to 3734 keV in $^{182}\text{W}$ . All known transitions are shown. See figure 11 for significance of dots and asterisks ..	33

13	The band structure assigned for states deduced in $^{182}\text{W}$ . The symbols $\pi$ and $\nu$ indicate whether proton or neutron single particle orbitals form the dominant configuration. Dotted levels indicate that the band assignment is tentative, and energies in parentheses indicate that the level is tentative .. .. ..	35
14	The even-parity bands observed in $^{182}\text{W}$ . Only the two most intense transitions associated with each level are shown. Refer to figure 13 for level energies .. ..	37
15	Coincidence spectra associated with the ground state band in $^{182}\text{W}$ .. .. .. .. .. ..	38
16	Coincidence spectra associated with the ground state band in $^{182}\text{W}$ (Contd.) .. .. .. .. .. ..	39
17	The excitation function for some $\gamma$ -rays observed in the $^{180}\text{Hf}(\alpha, 2n)^{182}\text{W}$ reaction. Normalization of the $14 \rightarrow 12$ points is arbitrary .. .. .. .. ..	40
18	A plot of $2J/\hbar^2$ vs. $\hbar^2\omega^2$ for the ground band of $^{182}\text{W}$ ..	41
19	A plot of energy vs. $I(I+1)$ for the ground and $K^{\pi} = 10^+$ bands in $^{182}\text{W}$ .. .. .. .. .. ..	43
20	$[E(I) - E(I-1)]/2I$ plotted vs. $2I^2$ for some rotational bands observed in $^{182}\text{W}$ .. .. .. .. ..	45
21	The diagram of Nilsson states for $^{182}\text{W}$ assuming deformation parameters of $\epsilon_2 = 0.235$ and $\epsilon_4 = 0.04$ . The Fermi surface is placed arbitrarily just above the orbitals known to form the ground state in neighboring odd- $A$ nuclei. Level energies not corrected for pairing.	53
22	The prompt and delayed coincidence spectra for the 518.5-keV gated transition .. .. .. .. ..	62
23	The prompt coincidence spectra associated with the $K^{\pi} = 10^+$ isomeric band .. .. .. .. ..	63
24	The odd parity band structure observed in $^{182}\text{W}$ . Only the two most intense transitions associated with each level are shown. Refer to figure 13 for level energies	66
25	$[E(I) - E(I-1)]/2I$ plotted vs. $2I^2$ for the $K^{\pi} = 2^-$ octupole band in $^{182}\text{W}$ .. .. .. .. ..	67

FIGURE	PAGE
26 The high-resolution $\gamma$ -ray singles spectrum associated with the decay of 64 h $^{182m}\text{Re}$ .. .. .. ..	75
27 Levels of $^{182}\text{W}$ populated in the decay of 64 h $^{182m}\text{Re}$ ..	79
28 Selected coincidence gates associated with $^{182m}\text{Re}$ decay	80

## I. INTRODUCTION

The ultimate goal of nuclear science is to determine the exact wavefunction for nuclei. While this is a goal which will almost certainly never be attained, it is possible that the forces acting within a nucleus that determine its properties can be understood. In search of this knowledge, many sophisticated experimental tools are available for the study of nuclear structure and properties, one such tool being  $\gamma$ -ray spectroscopy.

In the so-called deformed regions of nuclei, nuclear properties are strongly influenced by the existence of a static nuclear deformation. The degeneracy of the magnetic substates in a given "j" shell is split, and nuclear excitations resulting from rotation of the deformed system exist. It is of interest then to characterize the nuclear collective parameters so that intrinsic and coherent excitations can be understood. The use of in-beam  $\gamma$ -ray spectroscopy (i.e. the study of  $\gamma$ -ray spectra produced in the deexcitation of the compound nucleus produced in a nuclear reaction) is a technique which works very nicely for these studies, as levels associated with high spins not generally populated via  $\beta$ -decay can be investigated. On the other hand, the study of  $\gamma$ -ray spectra associated with  $\beta$ -decay can also be very useful, as the  $\beta$ -decay selection rules can provide information about excited nuclear states.

This thesis contains the results of a study of the deformed nuclei  $^{177}\text{Hf}$  and  $^{182}\text{W}$ , an investigation carried out via the techniques of radioactive decay and in-beam  $\gamma$ -ray spectroscopy, respectively. Some

properties of the intrinsic, vibrational, and rotational states in these nuclei are discussed, and the results of calculations are presented which describe the nuclear excitations in terms of the accepted phenomenological models. Such a study is useful for defining the parameters in the models which describe nuclei, and for allowing systematics of nuclear properties to be investigated.

II. THE DECAY OF  $^{177}\text{Ta}$  TO  $^{177}\text{Hf}$ 

## A. INTRODUCTION

Recent years have seen intense study of the odd neutron Hf and W isotopes because of the presence near the ground state of the positive parity states associated with the strongly mixed  $i_{13/2}$  family of Nilsson single particle orbitals. Much of this earlier work employed in-beam  $\gamma$ -ray spectroscopy, using primarily  $(\alpha, x\gamma\gamma)$  reactions on appropriate Yb or Hf targets. The study of the rotational band structure in such nuclei can yield significant information on the wave functions associated with the intrinsic single particle configurations. Such data are of special interest because of their apparent relevance to the phenomenon of "backbending" rotational structure recently observed in several even-even rare earth nuclei. Theoretical analysis of the perturbed rotational band structure in both odd- $A$  and even-even nuclei requires as much information as possible about the higher-lying perturbing Nilsson states and their associated rotational bands that mix into the lower-lying bands observed in the  $(\alpha, x\gamma\gamma)$  experiments. Such information on higher states can often be obtained from decay scheme studies.

The EC- $\beta^+$  decay of  $^{177}\text{Ta}$  to levels in  $^{177}\text{Hf}$  offers hope for a better understanding of at least one such case where the  $i_{13/2}$  single particle Nilsson orbits lie low in the quasiparticle spectrum; the high spin behavior of neighboring even-even isotopes should be directly influenced by the intrinsic configuration of these high- $j$  neutrons. The most recent  $^{177}\text{Ta}$  decay scheme is that proposed by West, Mann, and Nagle [We61] from their work using NaI(Tl) scintillation detectors. It thus seemed

reasonable to expect that Ge(Li) detectors might produce a considerable amount of new data on this decay. As we have recently published this work [Je74], a detailed account will not be given here. Instead, only a summary of the results will be included, and the reader is referred to [Je74] for details.

#### B. EXPERIMENTAL AND DISCUSSION

The  $^{175}\text{Lu}(\alpha, 2n)^{177}\text{Ta}$  reaction was carried out on a natural lutetium foil target to produce the 56.6-hr  $^{177}\text{Ta}$  activity. A solvent extraction technique was used to separate the Ta activity from the foil material, and  $\gamma$ -ray singles and  $\gamma$ - $\gamma$  coincidence data were taken with Ge(Li) detectors. A typical singles spectrum is shown in figure 1. The coincidence data were employed to construct the decay scheme shown in figure 2. The measured  $\gamma$ -ray intensities were used along with previous conversion electron data [We61] to determine  $\gamma$ -ray multipolarities. Where necessary, theoretical conversion coefficients [HS68] were employed to deduce the beta-decay branching, and  $\log ft$  values were calculated using the tables of Gove and Martin [Go71].

The state at 1002.8 keV was tentatively assigned even parity on the basis of the conversion coefficient of the 256.9-keV  $\gamma$ -ray, and therefore would offer some prospect for association with the  $i_{13/2}$  family of Nilsson orbitals. The most likely candidate for this state is the  $5/2^+[642]$  Nilsson orbital and the  $\gamma$ -ray transitions to lower-lying states in the spectrum are consistent with this interpretation. Better conversion-

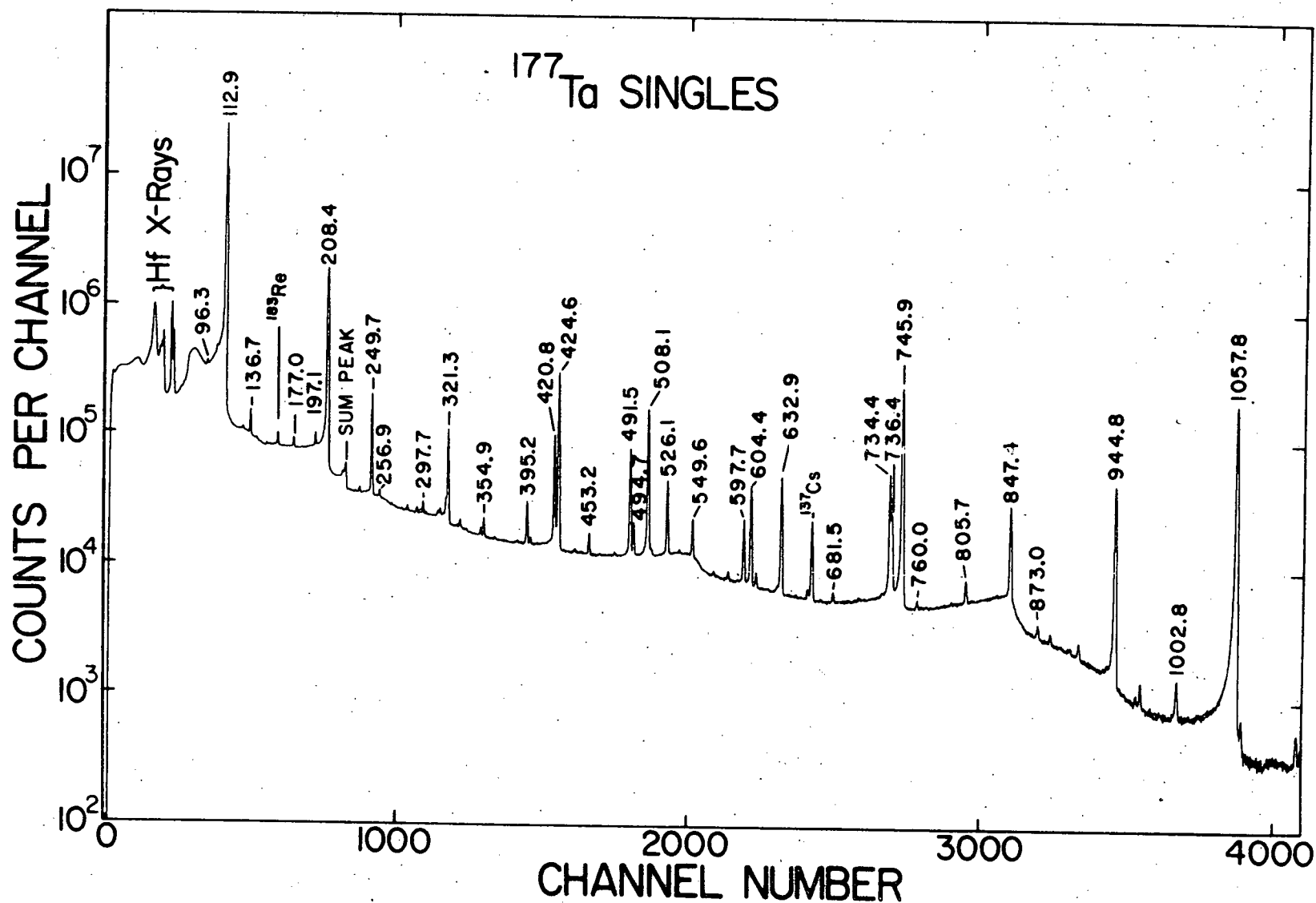


Figure 1. The  $\gamma$ -ray singles spectrum of  $^{177}\text{Ta}$ . A Cd-Cu absorber was used to attenuate the intense x-rays and 113-keV transition.

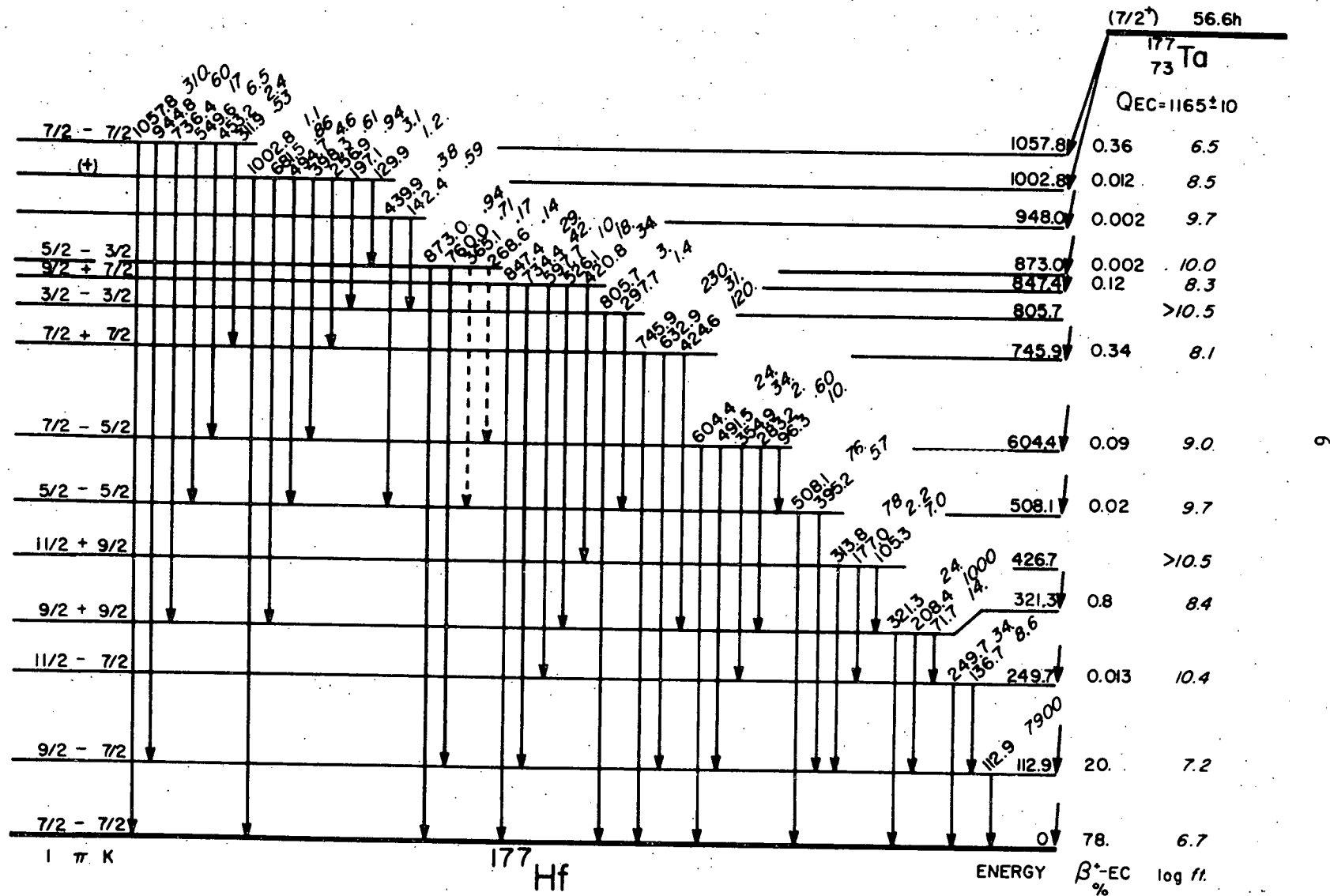


Figure 2. The  $^{177}\text{Ta}$  decay scheme. All transitions are placed on the basis of coincidence data except those associated with the 873 keV level.

electron data are needed to confirm this assignment, but the  $\log ft$  value associated with this state is consistent with it being  $5/2^+[642]$ ; the  $\log ft$ 's for both the  $9/2^+[624]$  and  $7/2^+[633]$  band heads are very similar to that of the 1002.8-keV state. All three  $\log ft$  values are quite high for "allowed"  $\beta$ -decay. This is not surprising, in view of the transition over two major oscillator shells required by the  $7/2^+[404] \rightarrow 5/2^+[642]$ ,  $7/2^+[633]$ ,  $9/2^+[624]$   $\beta$ -decay transformations.

In an attempt to determine whether the 1002.8-keV level was consistent with a  $5/2^+[642]$  state assignment, Coriolis calculations for mixing between the known band members from other  $i_{13/2}$  orbitals were carried out. The experimental input spectrum of states used in the calculation includes all members of the  $9/2^+[624]$  band known from  $^{177}\text{Lu}$  decay [Ha67] and the two members of the  $7/2^+[633]$  band confirmed in this study. With an appropriate selection of input parameters (cf. footnote e, Table 1), the complete Coriolis interaction matrix was constructed for each experimentally known spin state, and a best least squares fit to those energies was used as the basis for predicting the location of the  $5/2^+[642]$  state. The general method used has been summarized in [Je74].

Results of the calculations are shown in Table 1. It is seen that the energy fits (calculation I) to all known experimental data for even-parity states are quite good for reasonable values of  $\hbar^2/2J$  and  $B$ , and for the Nilsson single-particle energies defined by deformation parameters  $\epsilon_2 = 0.25$  and  $\epsilon_4 = 0.05$ . The predicted location of the  $5/2^+[642]$  state is about 1400 keV, however, considerably higher in energy than the 1002.8-keV candidate.

Table 1

Results of Coriolis-Mixing Energy Fit for Even-Parity States in  $^{177}\text{Hf}$ 

$I\pi(K)$	Experimental Energy	Fit I <sup>e</sup>	Fit II <sup>f</sup>
$5/2 + 5/2$	(1002.8)	1401.3	1002.9
$7/2 + 7/2$	745.9	745.9	746.2
$9/2 + 7/2$	847.4	847.4	847.6
$13/2 + 7/2$	1101 <sup>a</sup>	1101	1100
$9/2 + 9/2$	321.3	321.3	323.9
$11/2 + 9/2$	426.6 <sup>b</sup>	426.6	425.7
$13/2 + 9/2$	555.1 <sup>b</sup>	555.0	552.9
$15/2 + 9/2$	708.4 <sup>b</sup>	708.3	706.3
$17/2 + 9/2$	882.8 <sup>b</sup>	882.7	882.9
$19/2 + 9/2$	1086.9 <sup>b</sup>	1086.9	1086.7
$21/2 + 9/2$	1301.3 <sup>b</sup>	1301.3	1306.9
$23/2 + 9/2$	1560.9 <sup>c</sup>	1561.3	1558.2
<sup>d</sup> Deviation $\Sigma(\Delta E)^2 = 0.20$ $\Sigma(\Delta E)^2 = 58.2$			

<sup>a</sup>Ri68<sup>b</sup>Ha67<sup>c</sup>Hu73

<sup>d</sup> $\Sigma(\Delta E^2)$  is the sum of the squared deviations between experimental and calculated energies.

<sup>e</sup>Parameters adopted for this fit were:

$\hbar^2/2J = 15.6$  keV;  $B = -0.005$  keV;  $\Delta_n = 750$  keV;

$\lambda_n = 51.883$  MeV; *ad hoc* Coriolis reduction factors  $N_{\Omega, \Omega+1} = 0.99$ ,

0.80, 0.86, 0.66, 0.84, 0.99 for  $\Omega = 1/2$  through  $11/2$ . The quasi-

particle energy for the  $7/2^+[633]$  band head was decreased by 52 keV from theory.

<sup>f</sup>Parameters for this fit:  $\hbar^2/2J = 16.0$  keV;  $B = -0.01$  keV;

Table 3 (Contd.)

$N_{\Omega, \Omega+1} = 0.96, 0.70, 0.58, 0.68, 0.88, 0.96$ . The  $5/2^+[642]$  quasiparticle energy was decreased unrealistically by 510 keV.

A second set of calculations (II) is also shown that assumes the 1002.8-keV state is predominantly  $5/2^+[642]$ . The fit in this case is considerably worse; it was necessary to decrease unrealistically the  $5/2^+[642]$  quasiparticle energy by 500 keV, and the Coriolis matrix elements also required unusually large attenuations in this fit. It was impossible to improve the situation by any reasonable choice of deformation parameters.

These calculations do not lend strong support to the  $5/2^+[642]$  assignment for the 1002.8-keV level. It is possible to imagine seniority three states which could have the indicated even parity for this state, and one can even postulate states at this energy which could be formed by coupling octupole vibrations with the  $7/2^-[514]$  or  $5/2^-[512]$  single particle states. The possibility that this state may be odd parity also cannot be dismissed until more detailed conversion electron or transfer reaction data are available.

The remaining levels in  $^{177}\text{Hf}$  populated by  $^{177}\text{Ta}$  decay are for the most part well-characterized. Members of the rotational band based on the  $7/2^-[514]$ (gnd.),  $9/2^+[624]$ (321.3-keV),  $5/2^-[512]$ (508.1-keV), and  $7/2^+[633]$ (745.9-keV) states are known from previous work and are confirmed in this decay investigation. The level at 805.7 keV was found by Rickey and Sheline[Ri68] to be strongly populated in  $^{176}\text{Hf}(d,p)$ , and to have an angular distribution consistent with its assignment as the  $3/2^-[512]$  band head. The  $\gamma$ -ray deexcitation pattern from this state, and the log  $ft$  value from  $^{177}\text{Ta}$  decay to this state support the assignment.

The  $\gamma$ -ray singles spectrum of  $^{177}\text{Ta}$  also contains weak lines which, on the basis of energy sums and differences, indicate a level at 873.0 keV. While the existence of this level was not confirmed by coincidence data, a level at 878 keV was seen by Rickey and Sheline and assigned as the  $5/2^-$  member of the  $3/2^-$ [512] band. Since the  $\log ft$  value and  $\gamma$ -ray deexcitation pattern determined in our decay study are consistent with this interpretation, the 873.0-keV level is believed to be correctly placed, and is presumed to belong to the  $3/2^-$ [512] band. It is tempting to assign the state at 948.0 keV to this band as well, but Rickey and Sheline identify a level at 979 keV which they assign instead as  $I^\pi K = 7/2^- 3/2[512]$ . Moreover, the energy spacing between our 948-keV level and the  $5/2^-$  band member at 873.0 keV makes it most unlikely that the 948-keV state belongs to the same band, despite the  $\gamma$ -ray feeding into the  $3/2^-$ [512] band-head at 746 keV. (The expected strong Coriolis coupling between the  $3/2^-$ [512] and  $1/2^-$ [521] bands argues further against associating the 948-keV state with the  $3/2^-$ [512] band.)

Finally, the state at 1057.8 keV is assigned as  $7/2^-$ [503], also in agreement with the transfer reaction data. This assignment is consistent with the similar  $\log ft$  values to the ground and 1057.8-keV states, since the EC- $\beta^+$  decay transformations  $7/2^+[404] \rightarrow 7/2^-$ [514] or  $7/2^-$ [503] are both first-forbidden unhindered in the asymptotic selection rules.

We conclude that probable Nilsson assignments can be made for most of the states populated in  $^{177}\text{Ta}$  decay. Though more precise conversion electron and perhaps transfer reaction data are needed to characterize

the states at 948.0 and 1002.8 keV, it is evident that such decay scheme studies provide valuable information on the ordering of the quasiparticle spectrum and thereby provide indirect information on nuclear deformations in this region.

III. THE IN BEAM  $\gamma$ -RAY STUDY OF  $^{182}\text{W}$ 

## A. INTRODUCTION

The level structure of  $^{182}\text{W}$  has been investigated extensively through  $\beta$ -decay and transfer reaction studies, but has not been studied via in-beam  $\gamma$ -ray spectroscopy (except for a half-life measurement of an isomeric state [No71]). Because the  $(\alpha, 2n)$  reaction can transfer twelve or more units of angular momentum, it was thought that in-beam  $\gamma$ -ray spectroscopy would yield significant new information on the band structure of intrinsic and collective states in  $^{182}\text{W}$ . The study of this nucleus is of interest for several reasons. A number of high- $\Omega$  orbitals are expected to lie near the Fermi surface in  $^{182}\text{W}$ . These should give rise to several low-lying high- $K$  two-quasiparticle states, some of which are expected to be isomeric, since decay to the ground state band would be  $K$ -forbidden. One such isomer earlier identified was characterized in this work.

The study of  $^{182}\text{W}$  is also valuable because there is potential for understanding the interactions between the  $\beta$ - and  $\gamma$ - vibrational bands. These bands are strongly mixed, but previous empirical band-mixing calculations performed by Günther *et al.* [Gü71] suffered from a lack of experimentally known states. It was hoped that this work would establish the vibrational states to higher spins, and allow more definitive calculations to be done.

And finally, a study of this sort is valuable in extending the

systematics of nuclear properties in this region. To gain an understanding of recent problems in nuclear physics, such as the backbending recently seen in this region [Wa73], or the anomalous hexadecapole moments measured by Bemis *et al.* [Bem73], a detailed knowledge of the systematics of intrinsic and collective nuclear properties may be very valuable.

As a by-product of this project, the analysis of the in-beam data indicated that several errors existed in the accepted decay scheme for  $^{182m}\text{Re}$ . Therefore a short section on  $^{182m}\text{Re}$  decay has been included at the end of this thesis.

## B. EXPERIMENTAL

A number of experiments were conducted in the course of this study. These included  $\gamma$ -ray singles,  $\gamma$ - $\gamma$  coincidence, excitation function, angular distribution, and lifetime measurements. The excitation function and angular distribution measurements, however, were found to yield little new information because of difficulties in accurately resolving weak multiplets and because the multipolarities of many of the more intense  $\gamma$ -rays seen in-beam are known from the decay work of Galan *et al.* [Ga72] and Sapyta *et al.* [Sa70]. The  $\gamma$ -ray singles data were collected with a large volume Ge(Li) detector over a range of roughly 1800 keV, and with a smaller, high-resolution Ge(Li) detector over a range of  $\approx$  600 keV. The  $\gamma$ - $\gamma$  coincidence measurements were carried out using two

TABLE 2

Characteristics of Detectors Used in Study of  $^{182}\text{W}$ 

Size and Type <sup>a)</sup>	Resolution (FWHM) (keV)	Experiment
<1% Planar	0.6 at 122 keV	Singles
10.4% true coax	2.1 at 1333 keV	Singles and coincidence
7.7% true coax	1.9 at 1333 keV	Coincidence
10.3% true coax	2.0 at 1333 keV	Excitation function

a) Photopeak efficiency measured relative to a  $7.6 \times 7.6$  cm NaI(Tl) detector.

large Ge(Li) detectors. The characteristics of the detectors used are given in table 2. Half-life measurements were made by correlating the  $\gamma$ -rays from the target nuclei with the cyclotron beam bursts, a procedure described in more detail by Yamazaki *et al.* [Ya68]. Two half-life ranges were investigated: every beam burst was allowed to strike the target (period  $\sim 65$  ns), and the cyclotron beam sweeper was used so that only one beam burst in every nine struck the target (period  $\sim 0.6$   $\mu$ s).

### C. EXPERIMENTAL RESULTS

Figure 3 shows a typical  $\gamma$ -ray singles spectrum resulting from the  $^{180}\text{Hf}(\alpha, 2n)^{182}\text{W}$  reaction on a thin target prepared at the Niels Bohr Institute. The detector was placed at  $125^\circ$  with respect to the incident beam, and the beam energy was 26 MeV. The high resolution spectrum is shown in figure 4. The energies and intensities of  $\gamma$ -rays which could be assigned to the  $^{182}\text{W}$  level scheme from these data are given in table 3.

The  $\gamma$ - $\gamma$  coincidence data were taken at  $180^\circ$  geometry, using a thick chip of  $^{180}\text{Hf}$  metal supported by tantalum wire. The coincidence events were stored serially on magnetic tape for later analysis. The time information corresponding to each coincidence event was available in the form of a signal from a time-to-amplitude converter, and this information was also stored on the tape to allow subtraction of random events, and to make it possible to obtain delayed coincidence information for isomeric transitions. The resolving time for the prompt coincidence gates was  $\sim 75$  ns. The integral  $\gamma$ -ray spectra obtained from the experiment

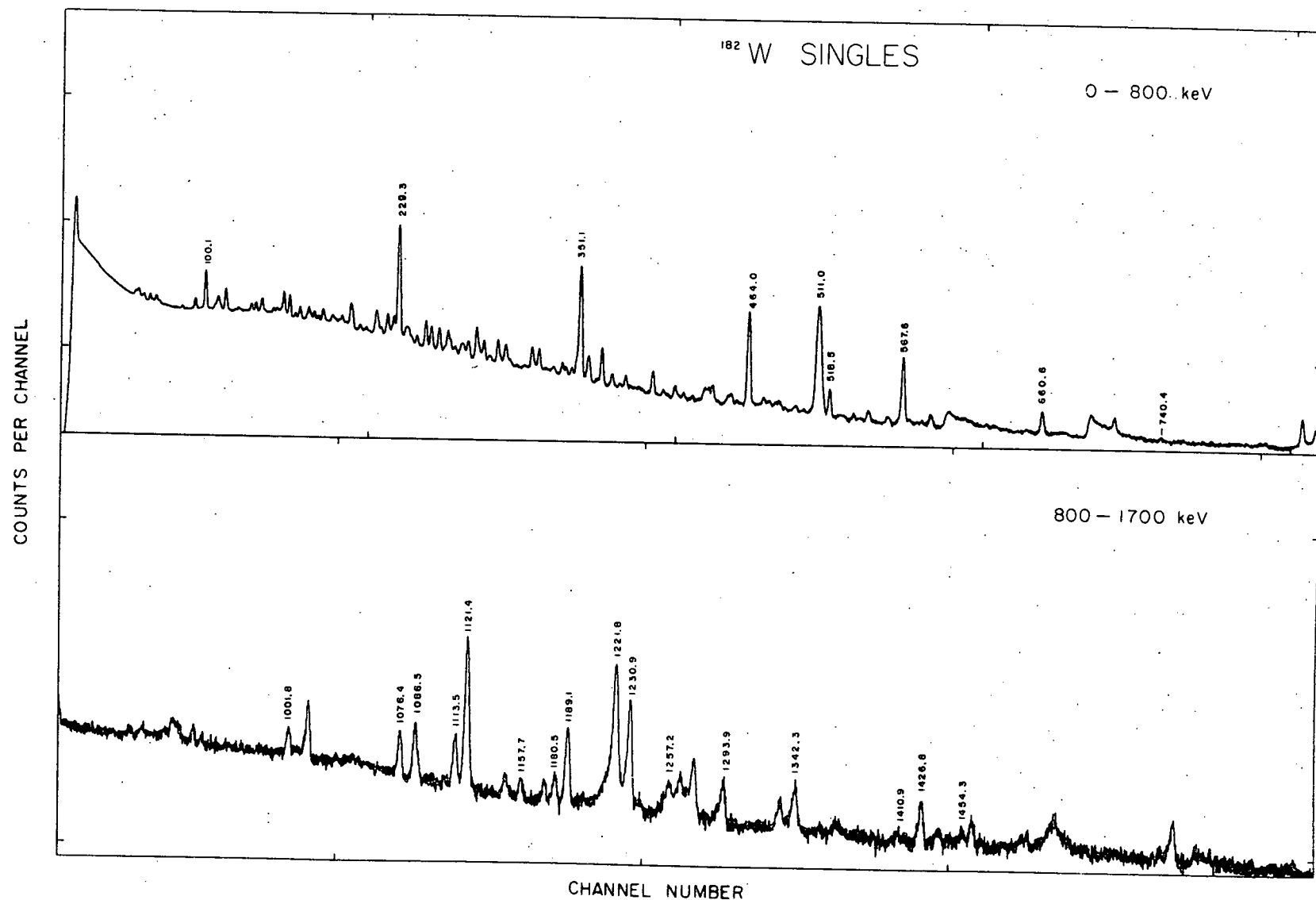


Figure 3. The in-beam  $\gamma$ -ray singles spectrum resulting from the  $^{180}\text{Hf}(\alpha, 2n)^{182}\text{W}$  reaction.

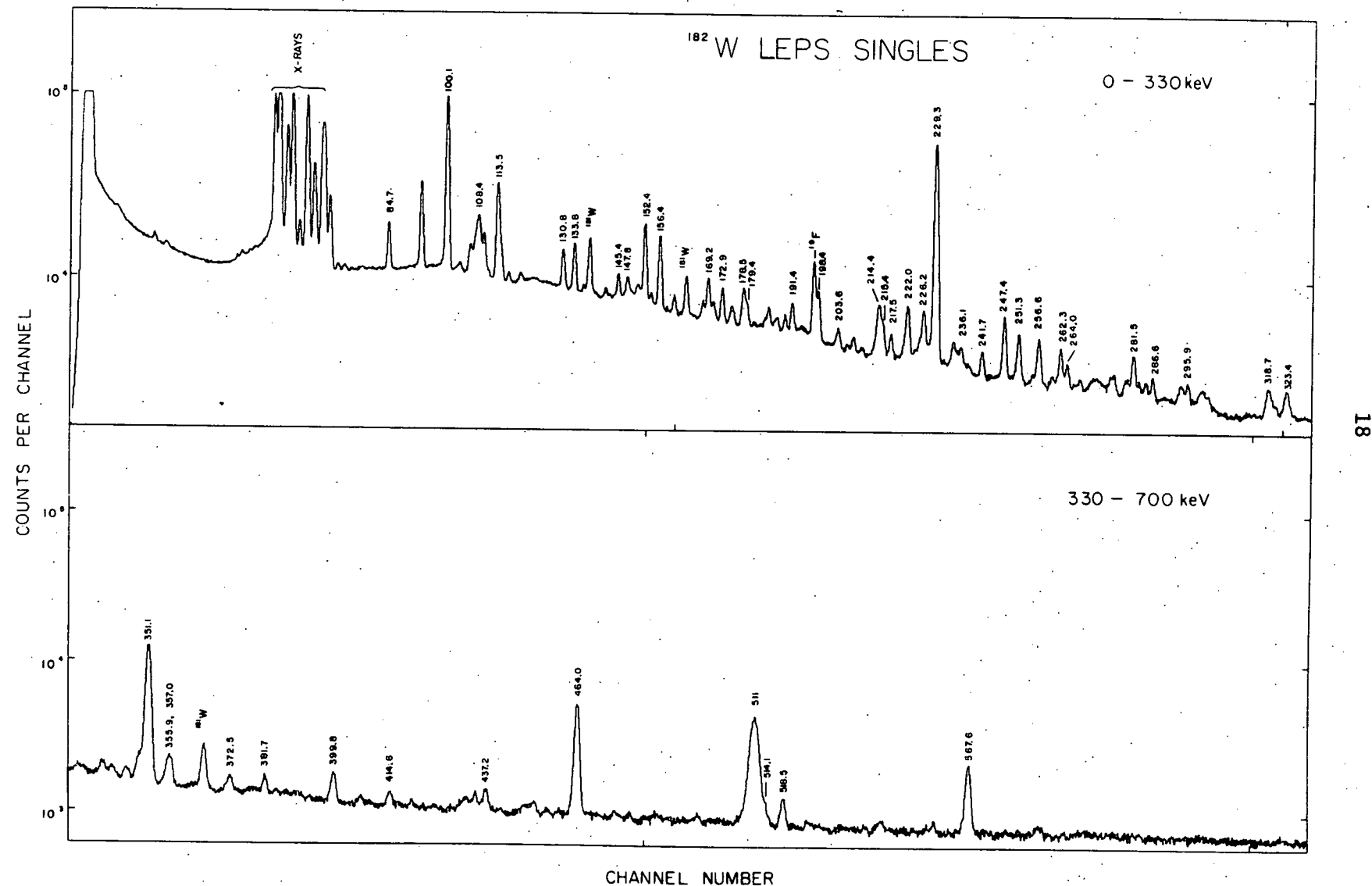


TABLE 3  
 $\gamma$ -Rays Observed Following the  $^{180}\text{Hf}(\alpha, 2n)^{182}\text{W}$  Reaction at 26 MeV.

$E_\gamma$ (keV) <sup>a</sup>	$I_\gamma$ <sup>b</sup>	Assignment	Multipolarity <sup>c</sup>
84.7	38 (3)	$1373.8 \rightarrow 1289.2$	M1 + E2
100.1	350 (30)	$100.1 \rightarrow 0$	E2
107.0 (2)	11.9 (0. )	$1660.4 \rightarrow 1553.2$	M1 + E2
108.4 (2)	40 (3)	$1769.0 \rightarrow 1660.4$	M1
111.1 (3)	4 (2)	$1621.3 \rightarrow 1510.2$	
113.5	106 (9)	$1487.5 \rightarrow 1373.8$	M1 + E2
116.4 (2)	5.4 (0.4)	$1373.8 \rightarrow 1257.4$	
130.8	31 (3)	$1960.3 \rightarrow 1829.5$	M1 + E2
133.8	41 (3)	$1621.3 \rightarrow 1487.5$	M1 + (E2)
145.4 (2)	23 (5)	$1769.0 \rightarrow 1623.5$	E1
147.8	25 (5)	$1769.0 \rightarrow 1621.3$	
148.9 (2)	7 (4)	$1978.4 \rightarrow 1829.5$	
150.2	11 (2)	( $1660.4 \rightarrow 1510.2$ )	
152.4	100 (10)	$1373.8 \rightarrow 1221.4$	E1
154.1	11 (2)	$2114.4 \rightarrow 1960.3$	
156.4	87 (7)	$1487.5 \rightarrow 1331.1$	E1
160.2	12 (1)	$2120.5 \rightarrow 1960.3$	
169.2	40 (3)	$1829.5 \rightarrow 1660.4$	M1
172.9	30 (3)	$1660.4 \rightarrow 1487.5$	M1
178.5	35 (3)	$1621.3 \rightarrow 1442.8$	E1
179.4	19.2 (1.5)	$1553.2 \rightarrow 1373.8$	M1 + E2

Table 3 (Contd.)

186.7 (2)	5.6 (0.8)	(1810.9 → 1623.5)	
189.6	12 (1)	1810.9 → 1621.3	
191.4	29 (2)	1960.3 → 1769.0	M1
198.4	53 (4)	1487.5 → 1289.2	E2
203.6	16.2 (1.3)	1960.3 → 1756.8	E2
206.1 (2)	4.6 (0.7)	1829.5 → 1623.5	
207.7	13.2 (1.1)	2328.0 → 2120.5	
209.9 (2)	5.0 (0.5)	(1978.4 → 1769.0)	(M1)
213.6 (2)	17.0 (3.0)	2328.0 → 2114.4	
214.4	54 (4)	1971.1 → 1756.8	M1
215.4	33 (3)	1769.0 → 1553.2	E2
217.5	20.3 (1.6)	1660.4 → 1442.8	E1
221.2 (2)	15.0 (1.5)	1978.4 → 1756.8	E1
222.0	64 (6)	1553.2 → 1331.1	E1
226.2	61 (6)	2204.5 → 1978.4	M1
229.3	1000. <sup>b</sup>	329.4 → 100.1	E2
236.1	21.2 (2.1)	2564.1 → 2328.0	
241.7	25.7 (2.1)	2212.8 → 1971.1	
247.5	79 (6)	1621.3 → 1373.8	E2
251.3	58 (5)	2455.8 → 2204.5	
256.6	56 (4)	1809.7 → 1553.2	M1
260.2	12.0 (1.0)	2824.3 → 2564.1	
262.3	46 (4)	2492.9 → 2230.6	

Table 3 (Contd.)

264.0	25.6 (2.0)	1553.2 $\rightarrow$ 1289.2	E2
267.4	8.3 (0.9)	2480.2 $\rightarrow$ 2212.8	
275.3 (2)	13.4 (1.3)	2731.1 $\rightarrow$ 2455.8	
276.4	19.0 (2.0)	1829.5 $\rightarrow$ 1553.2	E2
279.8 (3)	11.7 (2.3)	3104.1 $\rightarrow$ 2824.3	
281.5	51 (4)	1769.0 $\rightarrow$ 1487.5	E2
283.0	16.0 (2.0)	2775.9 $\rightarrow$ 2492.9	
286.6	22.0 (3.0)	1660.4 $\rightarrow$ 1373.8	E2
290.4 (2)	15.0 (3.0)	2770.6 $\rightarrow$ 2480.2	
295.9	25.0 (2.0)	1917.0 $\rightarrow$ 1621.3	
298.8	12.0 (3.0)	3029.9 $\rightarrow$ 2731.1	
299.8 (2)	19.0 (2.0)	1960.3 $\rightarrow$ 1660.4	
302 (1)	13 (5)	3077.1 $\rightarrow$ 2775.9	
313.6 (3)	4 (1)	1756.8 $\rightarrow$ 1442.8	
318.7	56 (5)	2087.7 $\rightarrow$ 1769.0	
320.2 (2)	11.0 (2.0)	3397.3 $\rightarrow$ 3077.1	
323.4	55 (5)	1810.9 $\rightarrow$ 1487.5	E2
339.1	27.8 (2.2)	1960.3 $\rightarrow$ 1621.3	E2
341.6	17.2 (1.4)	1829.5 $\rightarrow$ 1487.5	E2
345.4	22.4 (2.3)	2114.4 $\rightarrow$ 1769.0	
351.1	800 (60)	680.5 $\rightarrow$ 329.4	E2
355.9 (2)	32 (6)	2334.3 $\rightarrow$ 1978.4	
357.0 (2)	56 (8)	2274.0 $\rightarrow$ 1917.0	

Table 3 (Contd.)

362.4 (3)	13.0 (1.5)	2131.4 → 1769.0	
372.5	27.4 (2.2)	1993.8 → 1621.3	
399.8	56 (5)	2487.5 → 2087.7	
406.8 (2)	13.2 (5.0)	2323.8 → 1917.0	
414.6	26.6 (2.1)	2225.5 → 1810.9	
437.2	27.6 (2.2)	2711.2 → 2274.0	
452.3	21.2 (1.7)	2446.1 → 1993.8	
464.0	480 (40)	1144.5 → 680.5	
514.1 (3)	12 (3)	2739.6 → 2225.5	
518.5	63 (5)	2230.6 → 1712.1	
534.5	9.7 (0.9)	2980.6 → 2446.1	
558.2 (3)	8.5 (1.7)	2770.6 → 2212.8	
567.6	222 (18)	1712.1 → 1144.5	
586.2	21.3 (1.7)	3077.1 → 2492.9	
660.6	49 (4)	2372.7 → 1712.1	
740.1 (2)	6.5 (0.7)	3112.8 → 2372.7	
927.6 (2)	17.7 (1.8)	1257.4 → 329.4	E2
943.3 (4)	8.9 (1.8)	(1623.5 → 680.5)	
1001.8	35 (3)	1331.1 → 329.5	E2
1076.4	60 (5)	1756.8 → 680.5	
1086.5	73 (6)	2230.6 → 1144.5	
1113.5	56 (5)	1442.8 → 329.4	
1121.4	245 (20)	1221.4 → 100.1	E2

Table 3 (Contd.)

1157.7 (2)	23.3 (1.9)	1257.4 $\rightarrow$ 100.1	E0 + (M1) + E2
1180.5 (2)	32 (3)	1510.2 $\rightarrow$ 329.4	
1189.1	103 (8)	1289.2 $\rightarrow$ 100.1	E1 + M2 + E3
1221.8 (2)	166 (13)	1221.4 $\rightarrow$ 0	E2
1230.9	139 (11)	1331.1 $\rightarrow$ 100.1	
1257.2 (2)	34 (3)	1257.4 $\rightarrow$ 0	E2
1293.9 (2)	51 (4)	1623.5 $\rightarrow$ 329.4	
1342.3	52 (4)	1442.8 $\rightarrow$ 100.1	E2
1410.9 (5)	7.7 (1.6)	1510.2 $\rightarrow$ 100.1	
1426.8 (5)	51 (5)	1756.8 $\rightarrow$ 329.4	
1454.3 (3)	17.5 (1.9)	(1553.2 $\rightarrow$ 100.1)	

<sup>a</sup>Error is 0.1 keV unless otherwise indicated.

<sup>b</sup>Normalized to the 229.3-keV  $\gamma$ -ray. Errors in parentheses.

<sup>c</sup>Taken from Ga72.

are shown in figure 5. Weak contaminant  $\gamma$ -rays resulting from the tantalum wire and the  $^{180}\text{Hf}(\alpha, 3n)^{181}\text{W}$  reaction were present, but were easily identified from previous studies of these reactions [Li73, Hj68]. No contaminants from the  $^{180}\text{Hf}(\alpha, n)^{183}\text{W}$  reaction were identified. Because of the wealth of coincidence spectra generated from this experiment, only some of the more important gates are shown here, and these can be found in figures 6 through 10.

The lifetime measurements revealed only one isomeric state, located at 2230.6 keV, which decays into the ground band via transitions of 518.5 and 1086.5 keV. This isomer had already been observed by Nordhagen *et al.* [No71] to have a half-life of 1.4  $\mu\text{s}$ , and will be discussed in more detail in the section on positive-parity bands. The timing experiments make it possible to place an upper limit of 5 ns on the half-life of the other  $^{182}\text{W}$  levels populated in-beam.

#### D. CONSTRUCTION OF THE LEVEL SCHEME

The level scheme for  $^{182}\text{W}$  was deduced primarily from the coincidence data, and is shown in figures 11 and 12. Much of the level structure below 2 MeV was known from decay work [Ga72, Sa70], although several errors exist in these decay schemes. A difficulty encountered in the analysis was the existence of several very low energy transitions. The conversion electrons associated with these transitions were measured by Harmatz *et al.* [Ha61] and Ageev *et al.* [Ag70], and are placed in the level scheme on the basis of energy sums and differences, although some coincidence gates cannot be explained without them. In addition, some

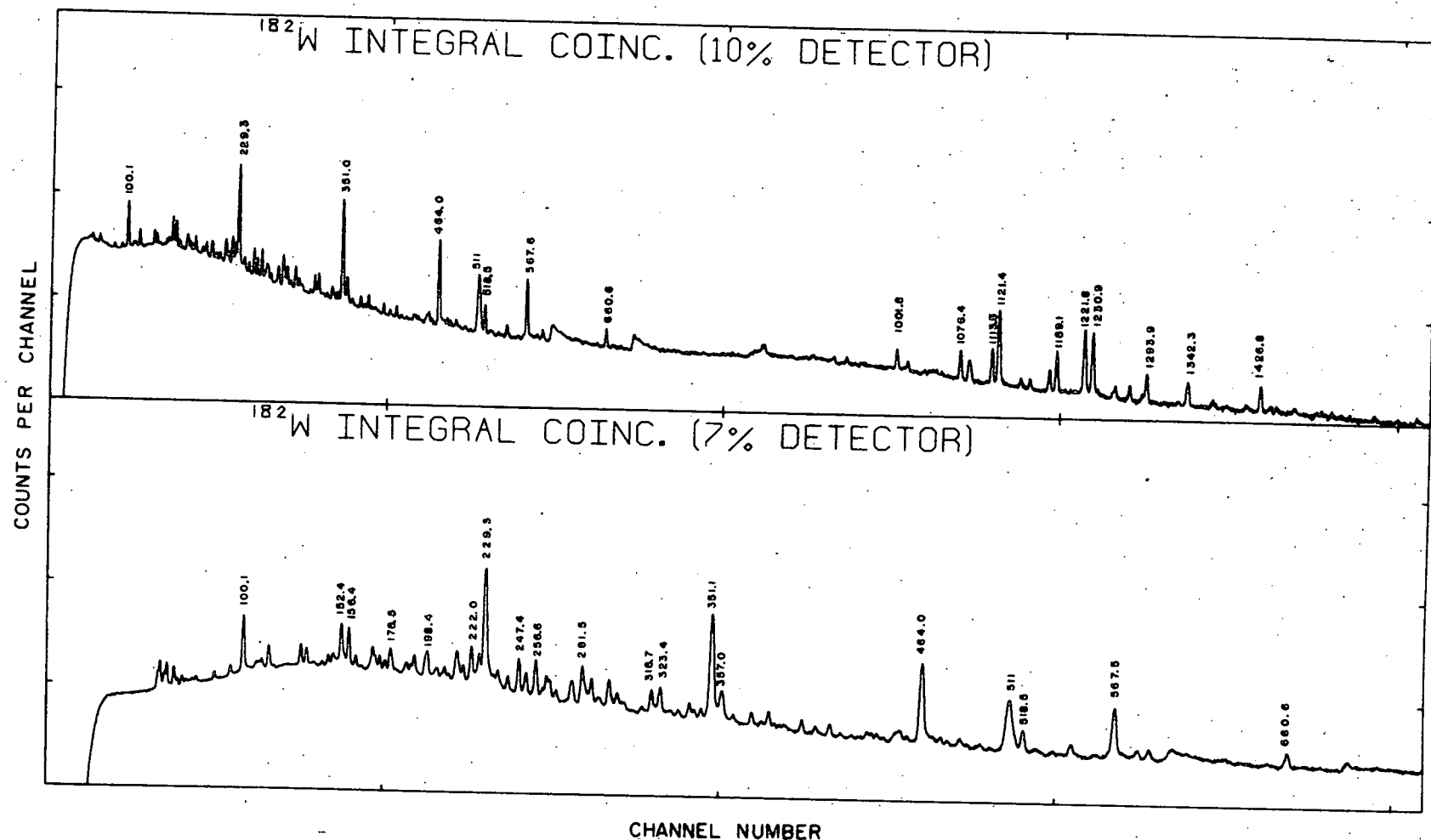


Figure 5. The integral coincidence spectra obtained for  $^{182}\text{W}$ .

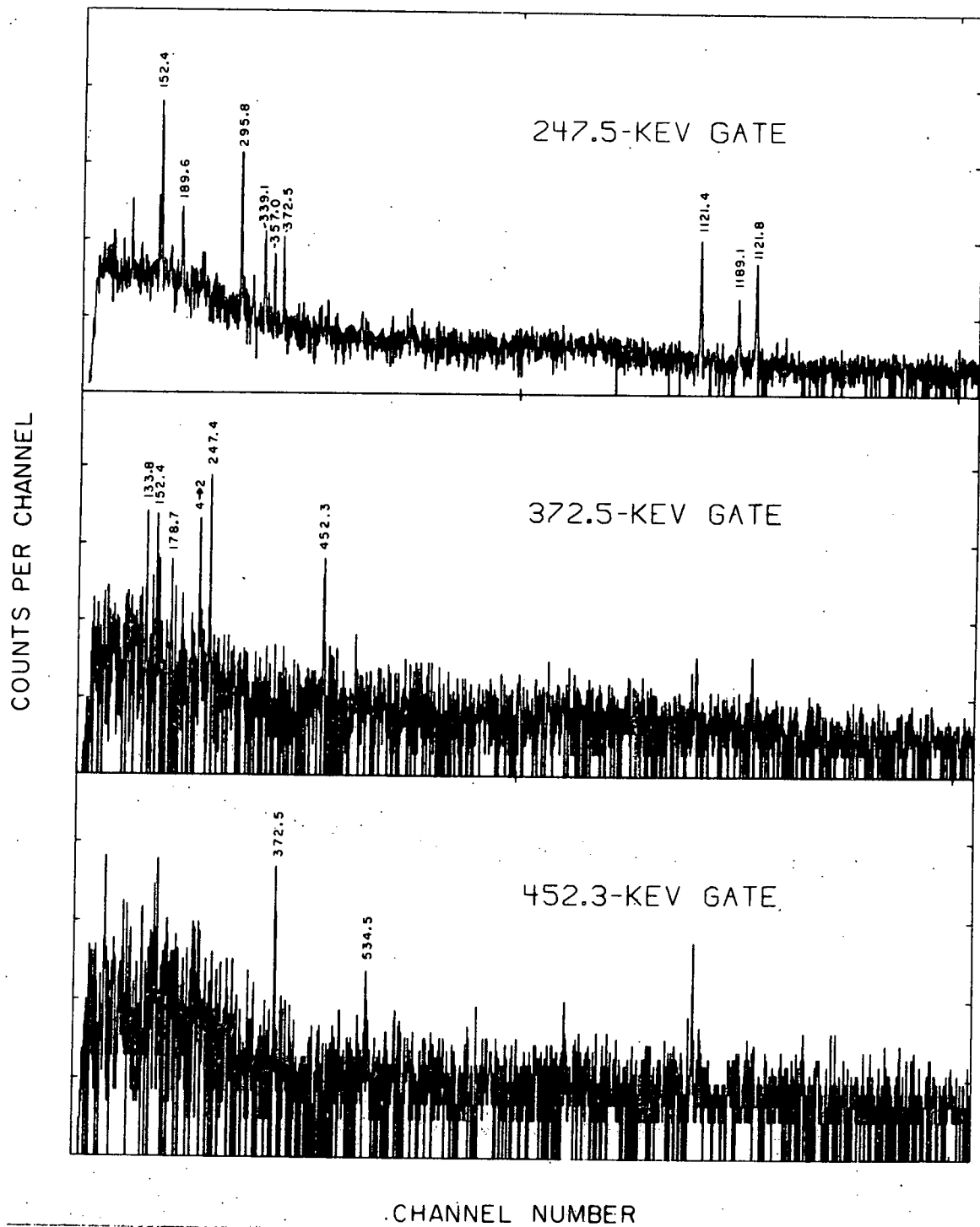


Figure 6. Coincidence gates associated with the  $K^{\pi} = 2^-$  octupole band.

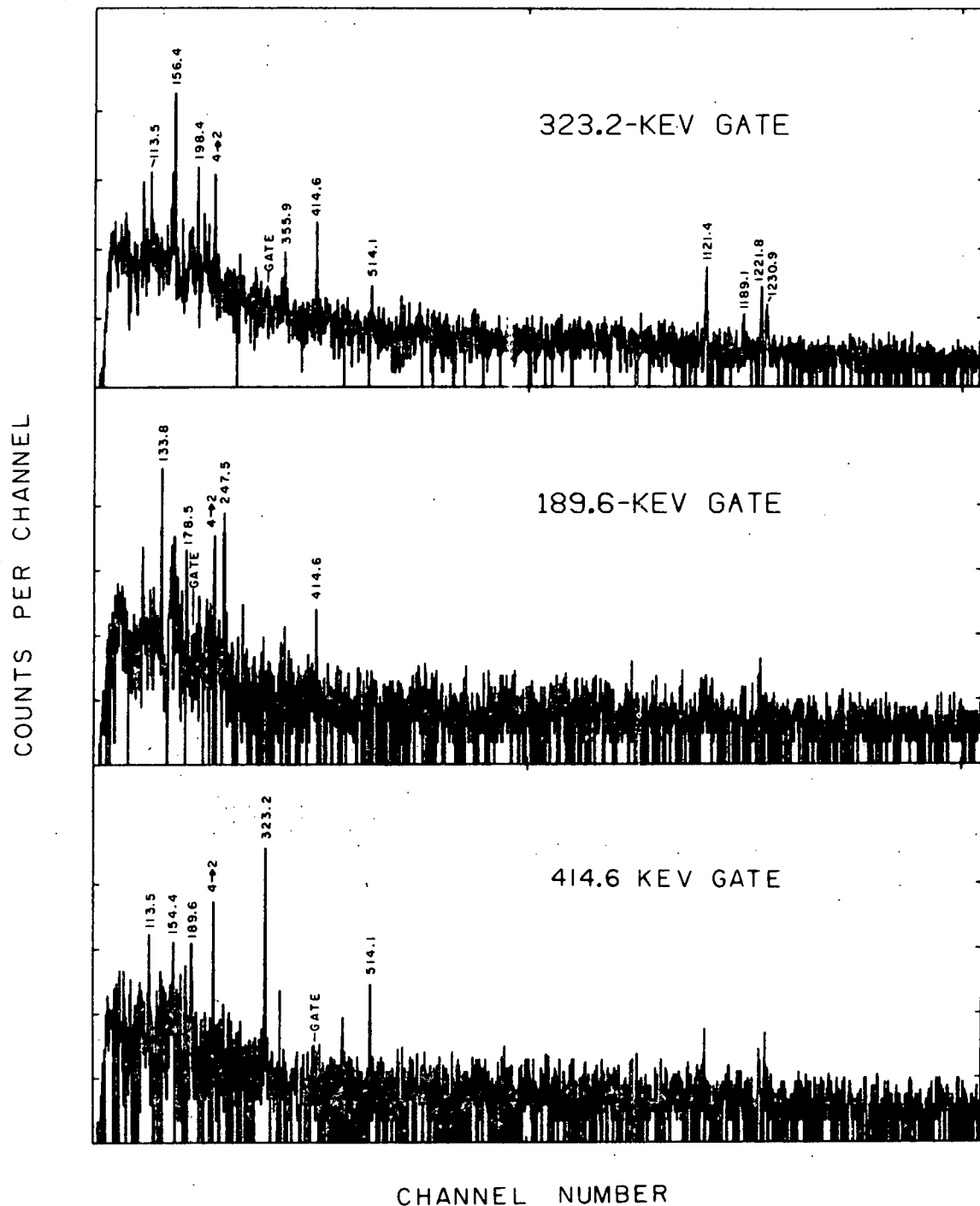


Figure 7. Coincidence gates associated with the  $K^\pi = 2^-$  octupole band.

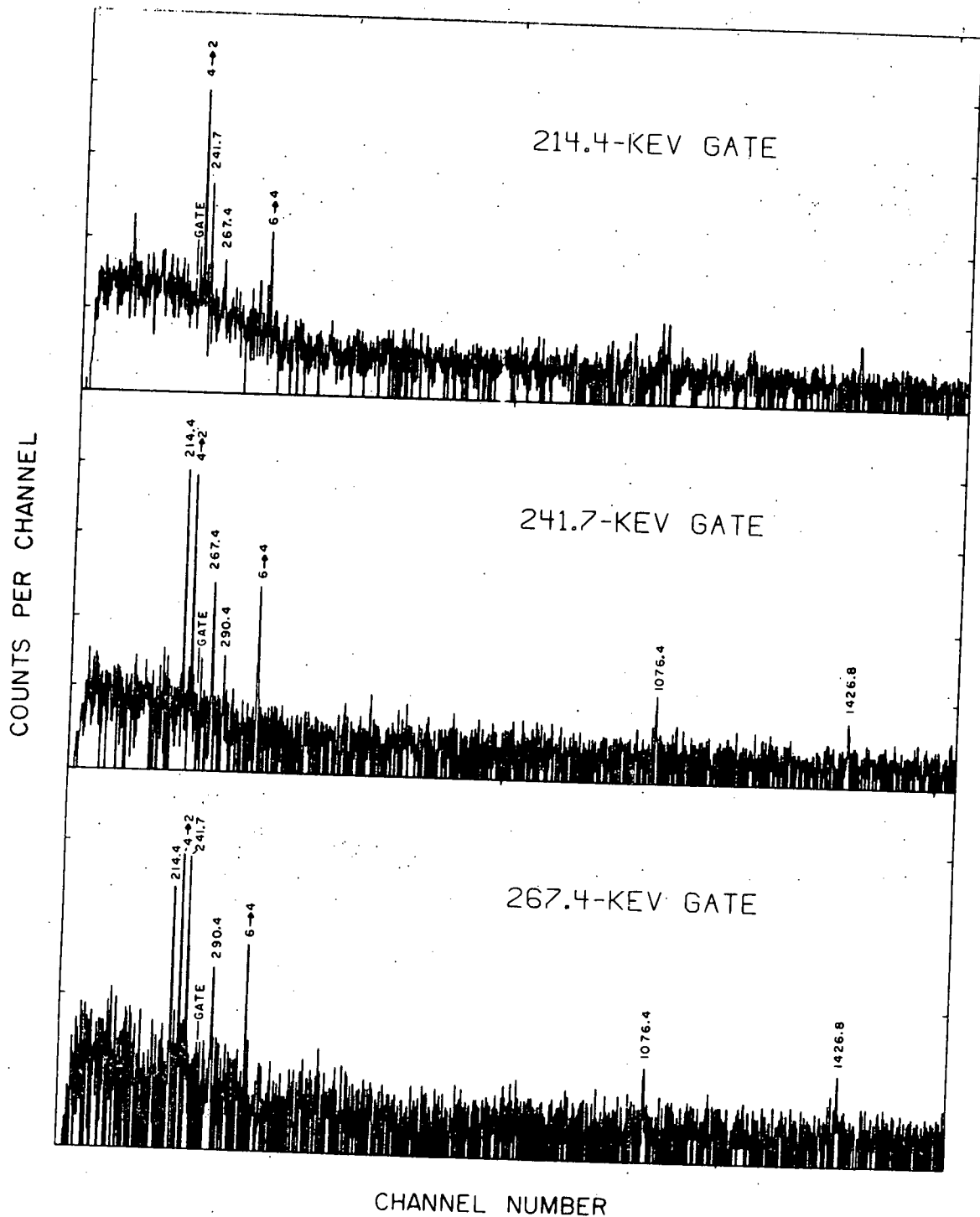
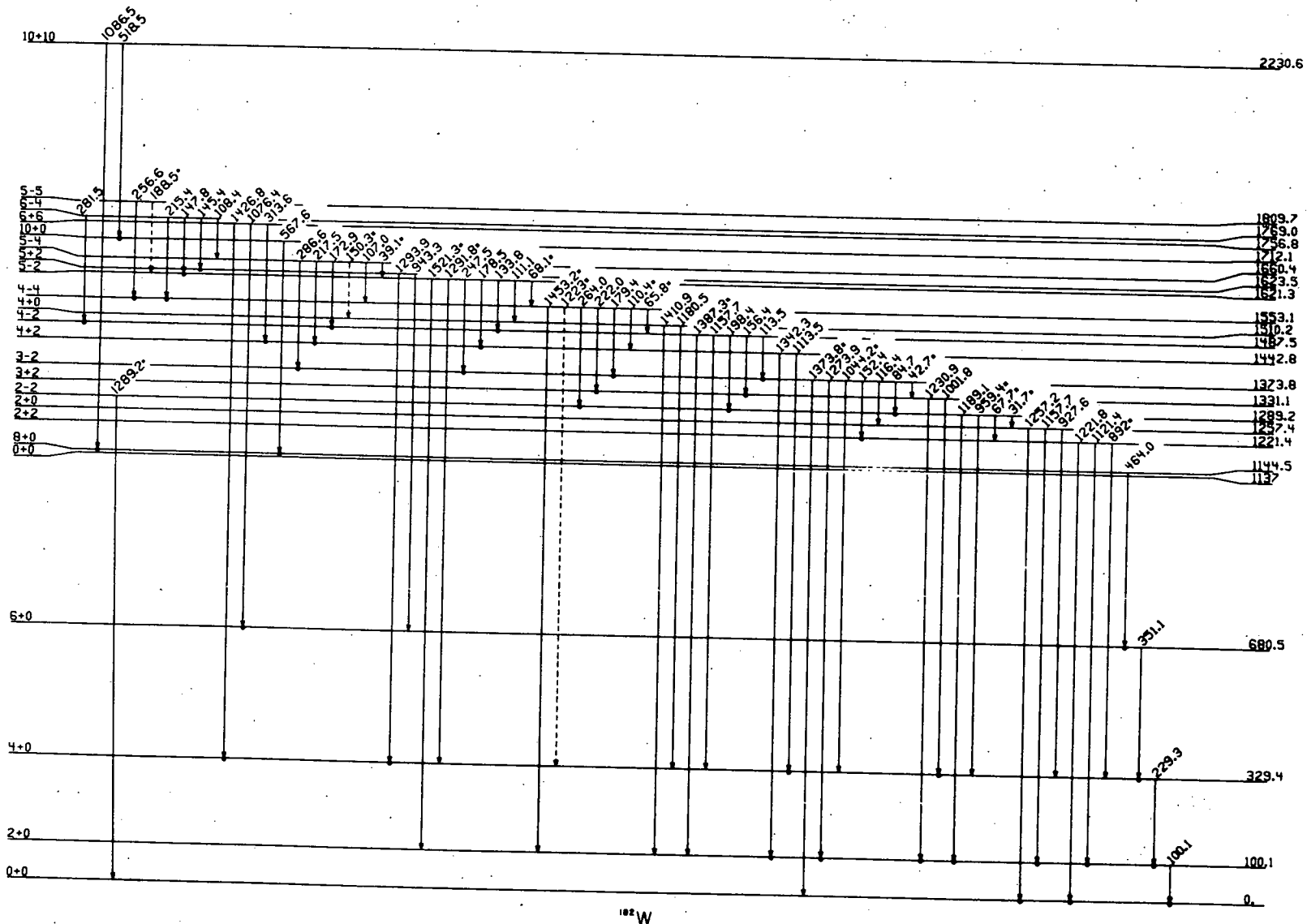


Figure 8. Coincidence gates associated with the  $K^\pi = 6^+$  bands.

Figure 11. A partial level scheme for states ranging from ground to 2230.6 keV in  $^{182}\text{W}$ . All known transitions are shown. Dots are below those transitions placed on the basis of coincidence data obtained in this study. Asterisks (\*) behind  $\gamma$ -ray energies indicate that the transition is known only from decay studies [Ha61, Sa70]. The level at 1137 keV is taken from Kleinheinz *et al.* [K173].



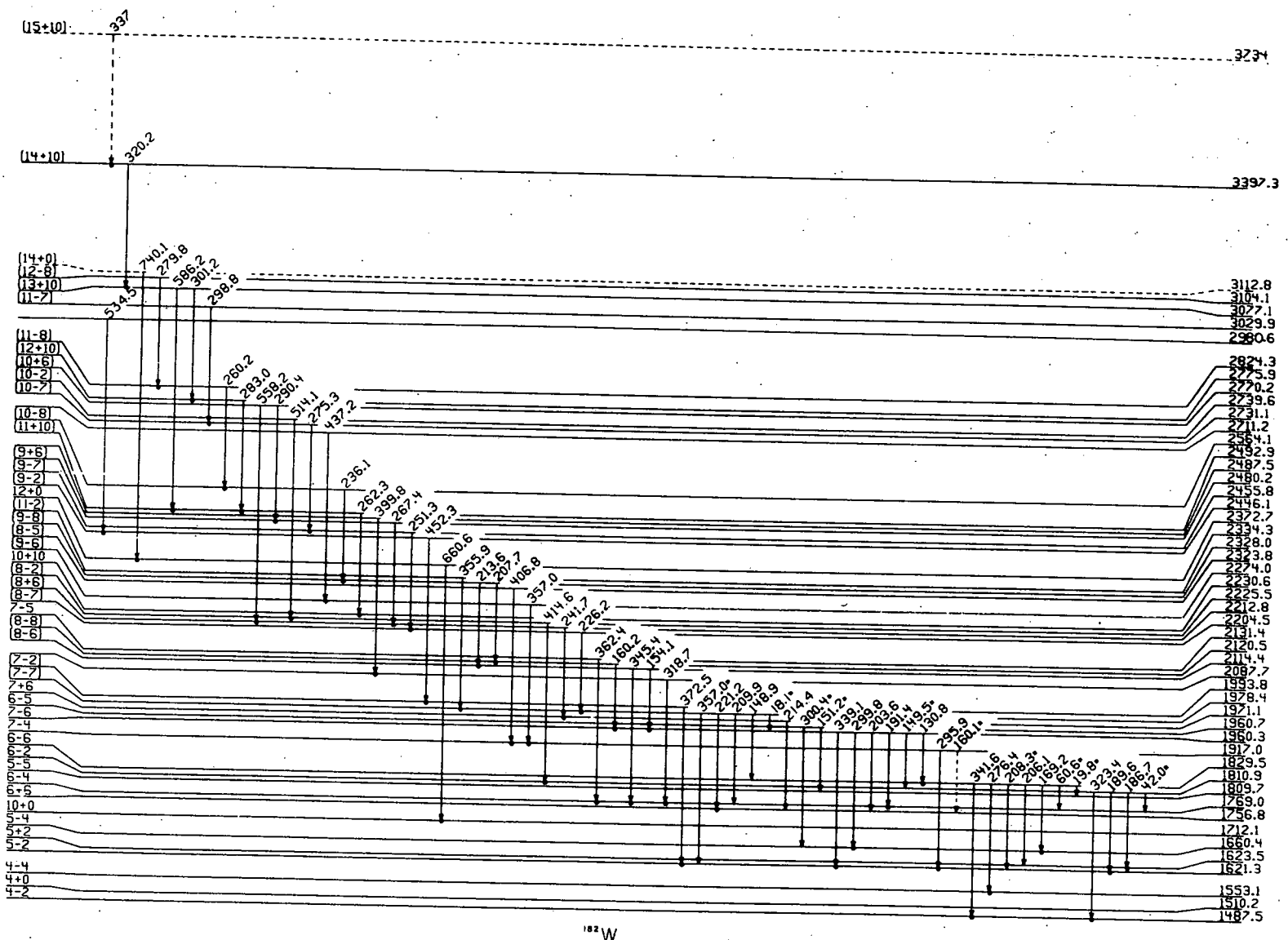


Figure 12. A partial level scheme for states ranging from 1487.5 keV to 3734 keV in  $^{182}\text{W}$ . All known transitions are shown. See Figure 11 for significance of dots and asterisks.

$\gamma$ -rays too weak to be seen in-beam are known to exist from  $^{182m}\text{Re}$  decay. For completeness, all transitions known to exist from the  $\gamma$ -decay of excited states in  $^{182}\text{W}$  are shown on the level scheme, but only the  $\gamma$ -rays actually seen in-beam are listed in table 3. The  $\gamma$ -rays which are placed on the basis of the in-beam  $\gamma$ - $\gamma$  coincidence data are indicated by dots underneath the arrows, and levels which were placed on the basis of weak coincidence evidence or energy sums and differences were dotted to indicate that the level assignment is tentative. All levels known from  $^{182m}\text{Re}$  decay are also populated in-beam with the possible exception of the 1960.7-keV state. As will be discussed in the section on  $^{182m}\text{Re}$  decay, this state is difficult to detect by coincidence techniques because of the intensity of  $\gamma$ -rays from the 1960.3-keV state. Experimental conditions in-beam make this state even more difficult to detect, so that it was impossible to determine through the coincidence measurements whether the state was being populated.

Spins and parities assigned in the level scheme are based on the assignments of [Ga72] and [K173]. When band structure could be extended beyond that seen in these references, spins were assigned based purely on the expected regular spin dependence of the band members, and are indicated as tentative on the level scheme.

A useful way to decompose the level scheme is to separate the states into rotational bands, and this has been done in figure 13. A large number of bands are populated in-beam, probably due to the large number of low-lying high-K states in the nucleus. The bands are constructed on the basis of  $\gamma$ -ray decay patterns, not shown in figure 13 due to the

## ROTATIONAL BANDS IN $^{182}\text{W}$

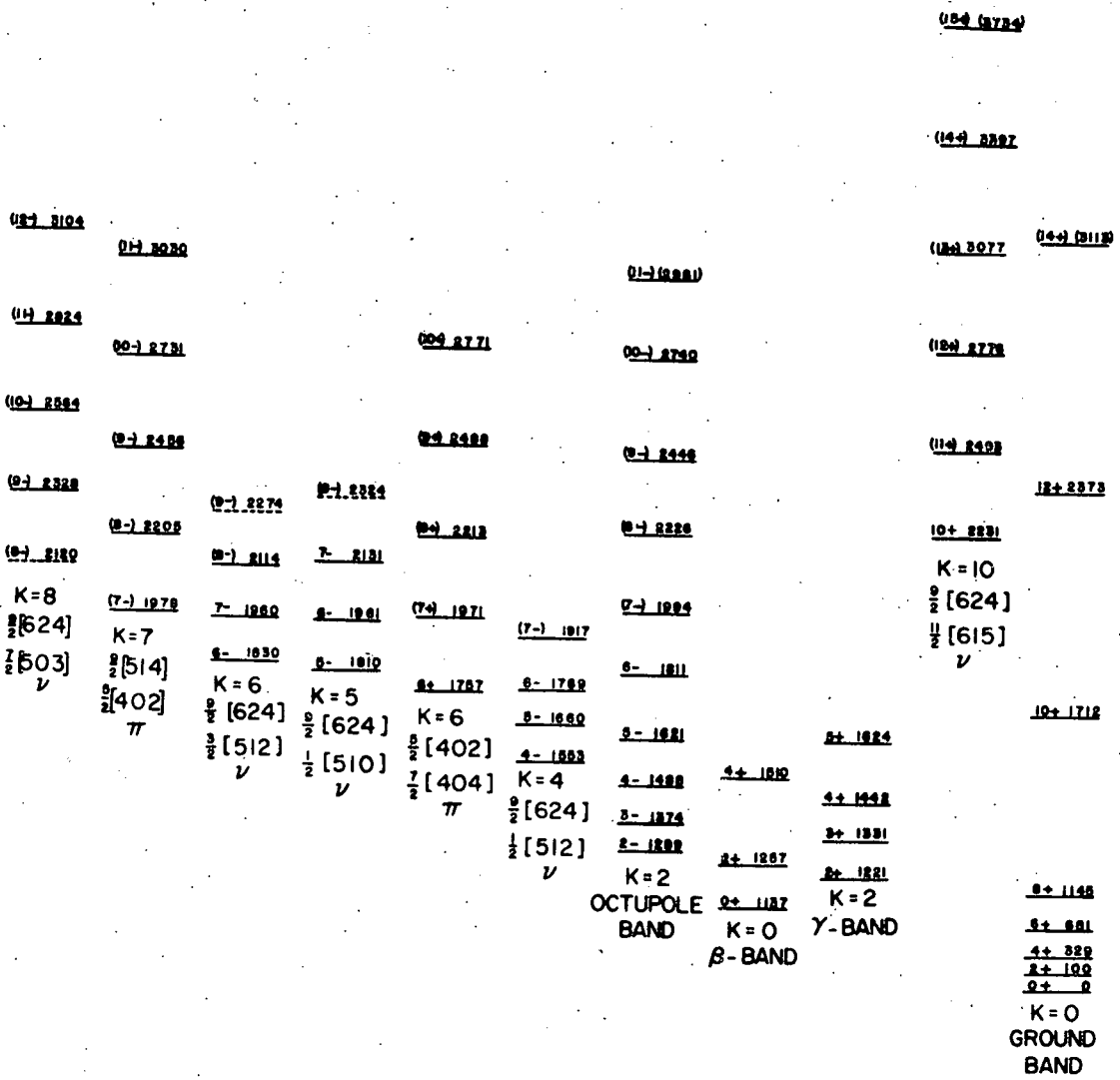


Figure 13. The band structure assigned for states deduced in  $^{182}\text{W}$ . The symbols  $\pi$  and  $\nu$  indicate whether proton or neutron single particle orbitals form the dominant configuration. Dotted levels indicate that the band assignment is tentative, and energies in parentheses indicate that the level is tentative.

complexity of the decay.

### 1. Even Parity Bands

There were five even parity bands observed in this study. From figure 13, these are seen to be the ground,  $\beta$ , and  $\gamma$  collective bands, a  $K^\pi = 6^+$  two-quasi-proton band, and the  $K^\pi = 10^+$  isomeric two-quasi-neutron band. A partial level scheme of these bands including the prominent  $\gamma$ -ray transitions is given in figure 14. The  $\beta$ - and  $\gamma$ -band assignments are taken from Kleinheinz *et al.* [K173].

Through the  $\gamma$ - $\gamma$  coincidence experiment we were able to establish the ground state rotational band definitely up to  $I = 12$ , and tentatively up to  $I = 14$ . The coincidence gates for this band are shown in figures 15 and 16. The  $14 \rightarrow 12$  transition at 740 keV is seen as a very weak line in the  $12 \rightarrow 10$  gate, and is even less apparent in the other gates. However, a  $\gamma$ -ray of this energy is definitely seen in singles, and the excitation function shown in figure 17 is in agreement with the  $14 \rightarrow 12$  assignment for this state. At 24 and 26 MeV, the 740-keV  $\gamma$ -ray could not be seen, but at the higher beam energies, the line became apparent. Since this  $\gamma$ -ray was not seen in  $^{181}\text{W}$  [Li73], the assignment as a transition from a high spin state seems justified. A plot of  $2J/\hbar^2$  vs.  $\hbar^2\omega^2$  for the ground band is shown in figure 18. The point associated with the tentative  $14^+$  state deviates slightly from the line defined by the other members of the band.

This nucleus presents a particularly interesting case for the study of backbending because of the identification of the  $K^\pi = 10^+$  two-quasi-

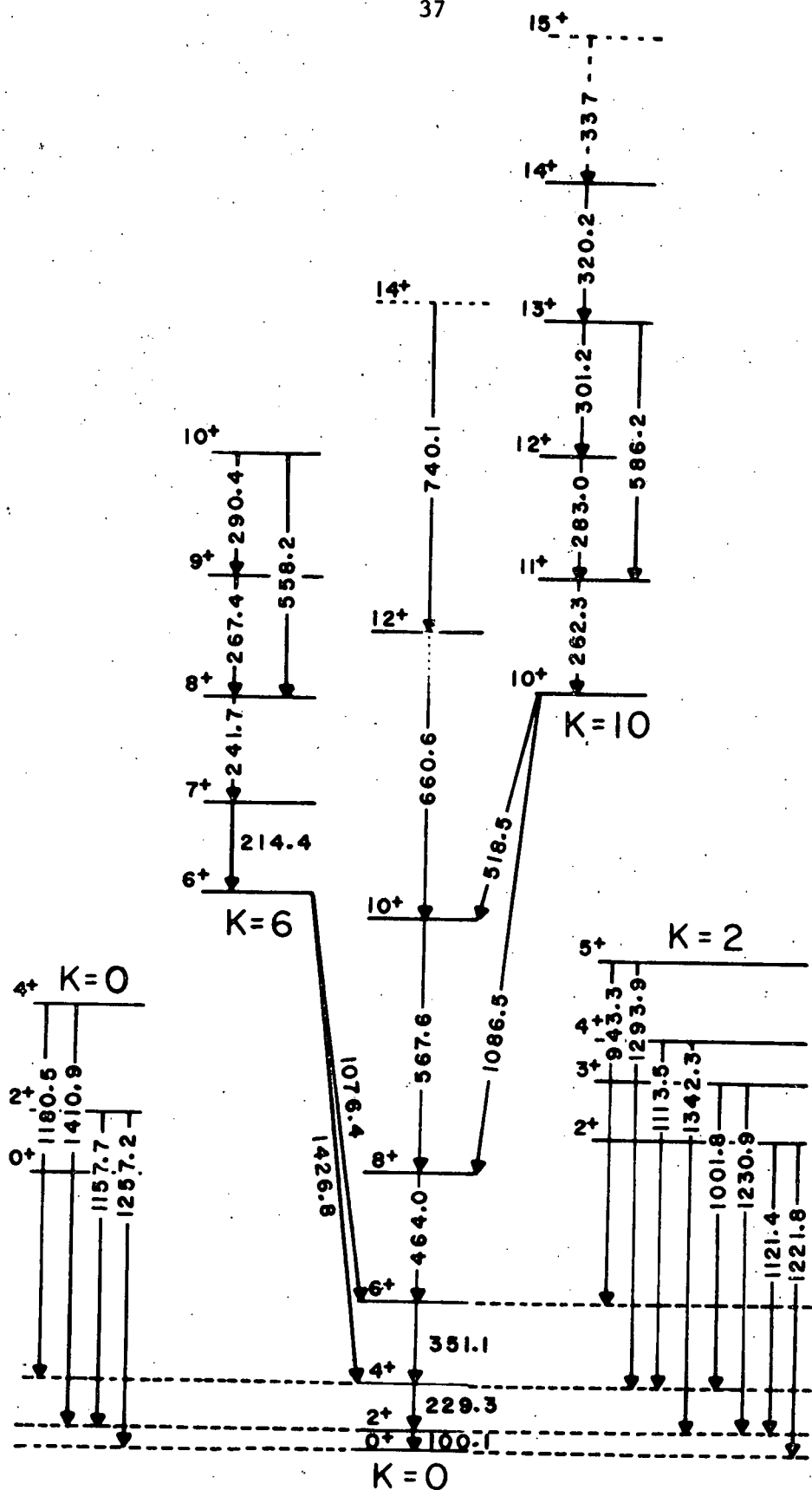


Figure 14. The even-parity bands observed in  $^{182}\text{W}$ . Only the two most intense transitions associated with each level are shown. Refer to figure 13 for level energies.

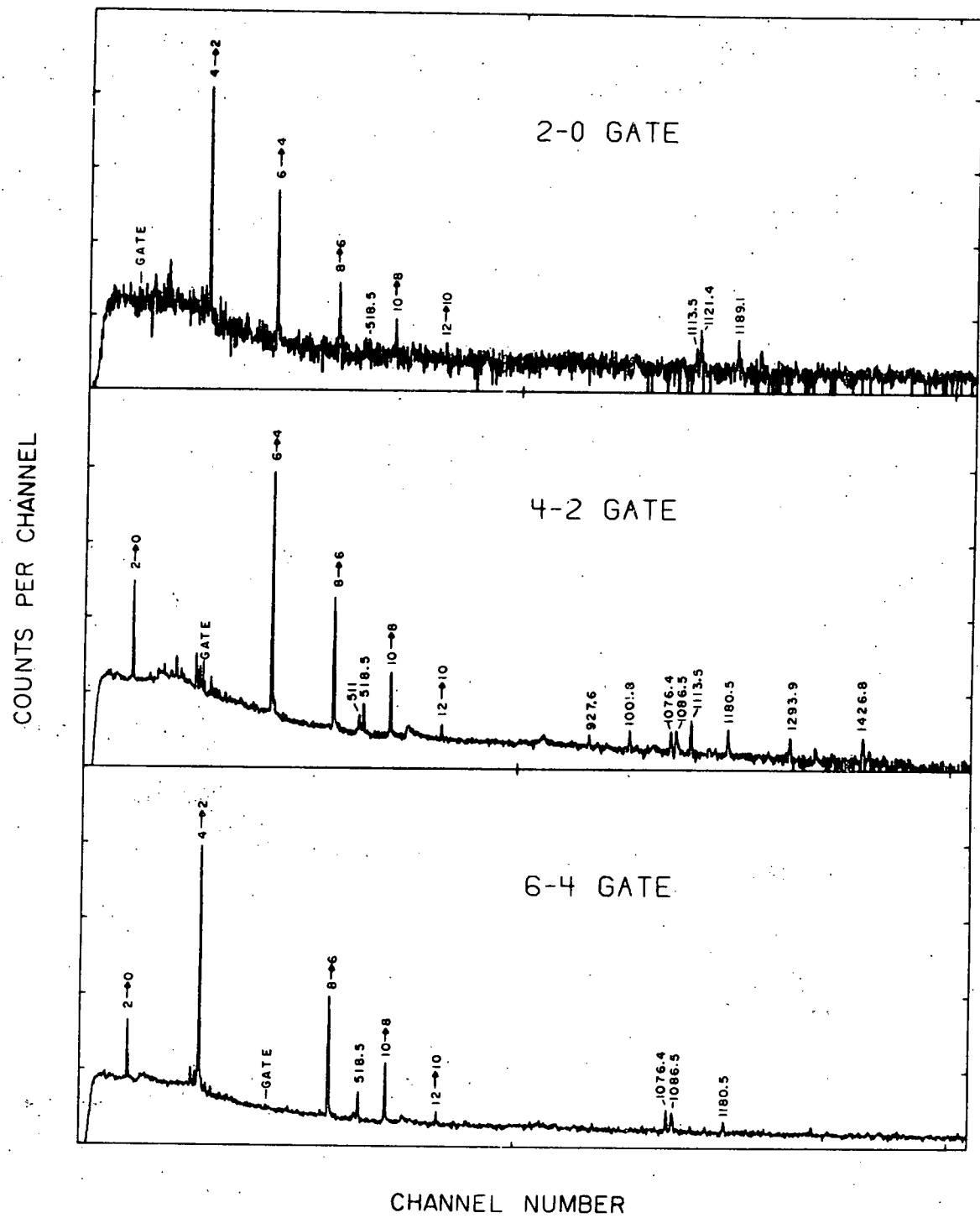


Figure 15. Coincidence spectra associated with the ground state band.

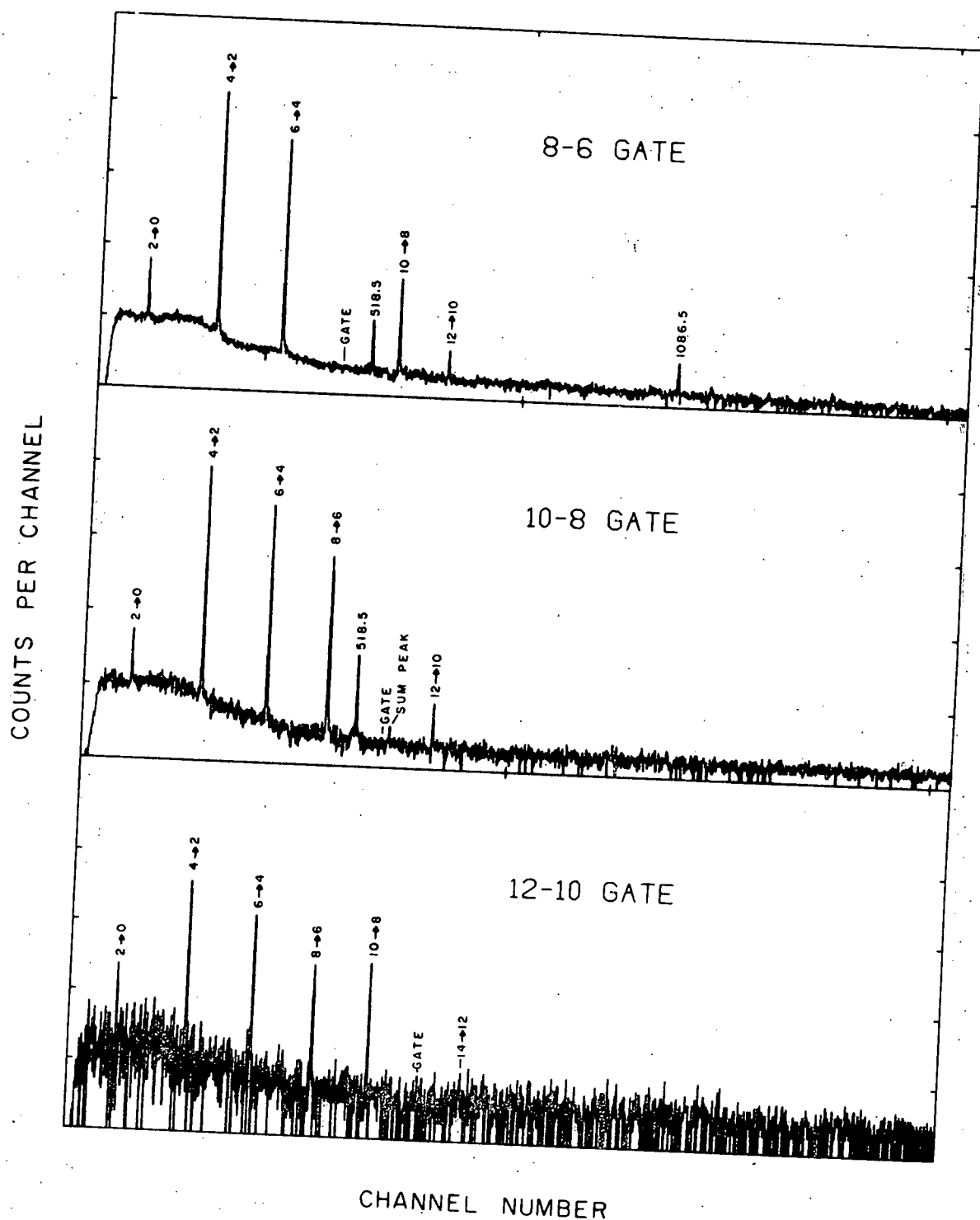


Figure 16. Coincidence spectra associated with the ground state band.

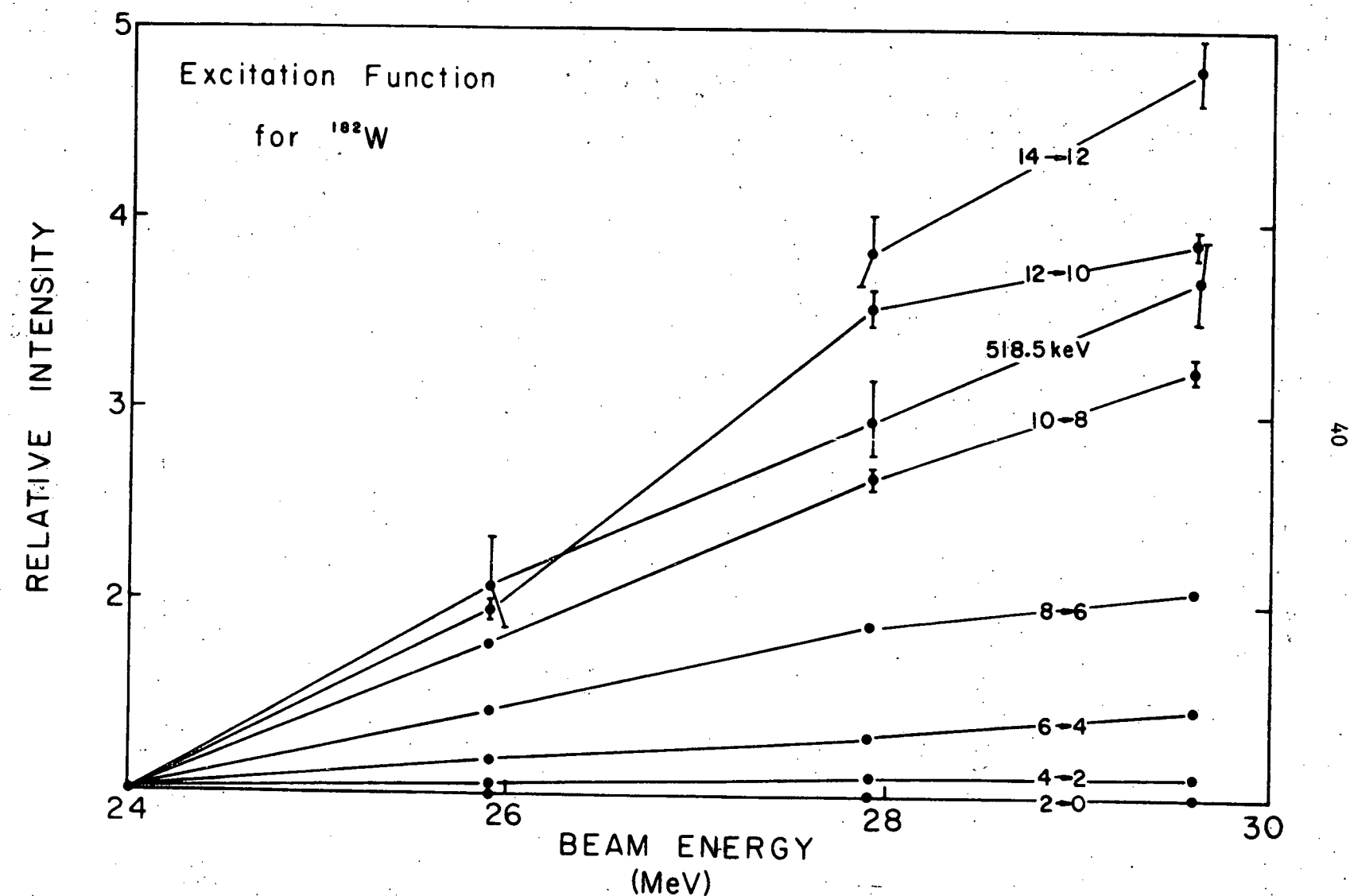


Figure 17. The excitation function for some  $\gamma$ -rays observed in the  $^{180}\text{Hf}(\alpha, 2n)^{182}\text{W}$  reaction. Normalization of the  $14 \rightarrow 12$  points is arbitrary.

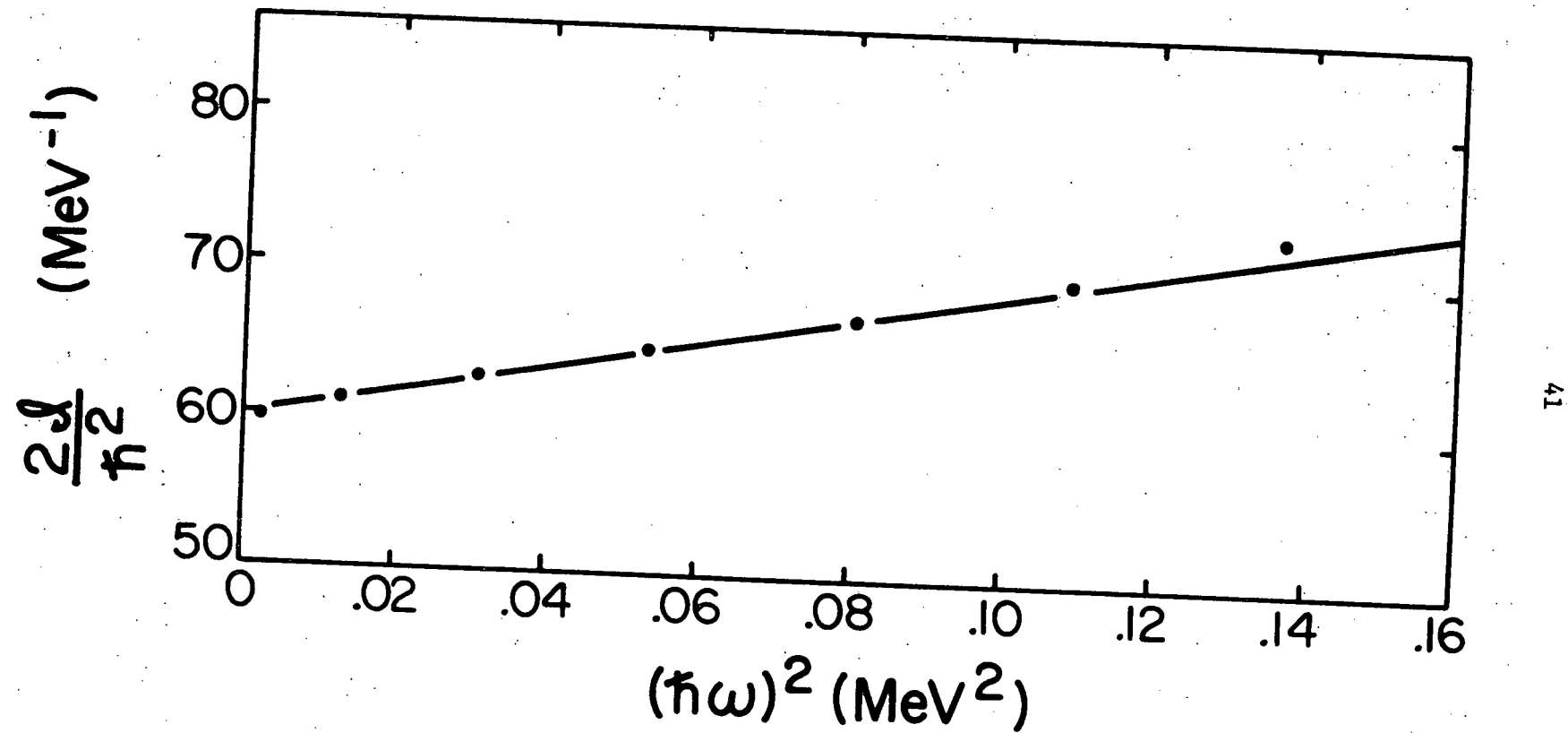


Figure 18. A plot of  $2J/\hbar^2$  vs.  $\hbar^2\omega^2$  for the ground band of  $^{182}\text{W}$ .

particle band. As will be discussed later, the intrinsic structure of this band is based on a triplet coupling of the  $\Omega = 9/2$  and  $\Omega = 11/2$   $i_{13/2}$  neutrons, and in the Stephens and Simon model, it is the  $i_{13/2}$  neutrons nearest the Fermi surface which would be involved in backbending in  $^{182}\text{W}$  [St72]. Figure 19 shows a plot of  $E$  vs.  $I(I+1)$  for the ground and  $K = 10$  bands, and it is apparent that the two bands should cross at about spin 16. At this point one might expect the two bands to become sufficiently mixed for prominent interband transitions to occur. In addition, backbending could occur in the ground band if the particles forming the  $K = 10$  band were to become sufficiently decoupled from the nuclear core. However, if the Stephens and Simon model holds, it is possible to predict that backbending should in fact not occur in  $^{182}\text{W}$ . This prediction rests on calculations of Bernthal [Be74a] in which the degree of decoupling is determined for the adjacent nucleus  $^{181}\text{W}$ . The calculations show that in  $^{181}\text{W}$  the  $i_{13/2}$  neutrons that could produce backbending behavior remain strongly coupled to the deformed nuclear core, even at relatively high spins. By implication, backbending should not occur in  $^{182}\text{W}$ .

The fact that the  $K = 10$  state in  $^{182}\text{W}$  is a 1.4  $\mu\text{sec}$  isomer, and the band structure associated with the isomer remains relatively unperturbed to spin 15 at least, indicates this expectation is borne out. It would be most interesting to examine the behavior at the spin-16 band-crossing point, for one could then hope to extract matrix elements for mixing of the g.r.b. and the  $K = 10$  band if interband  $\gamma$ -ray transitions were indeed observed. However this possibility

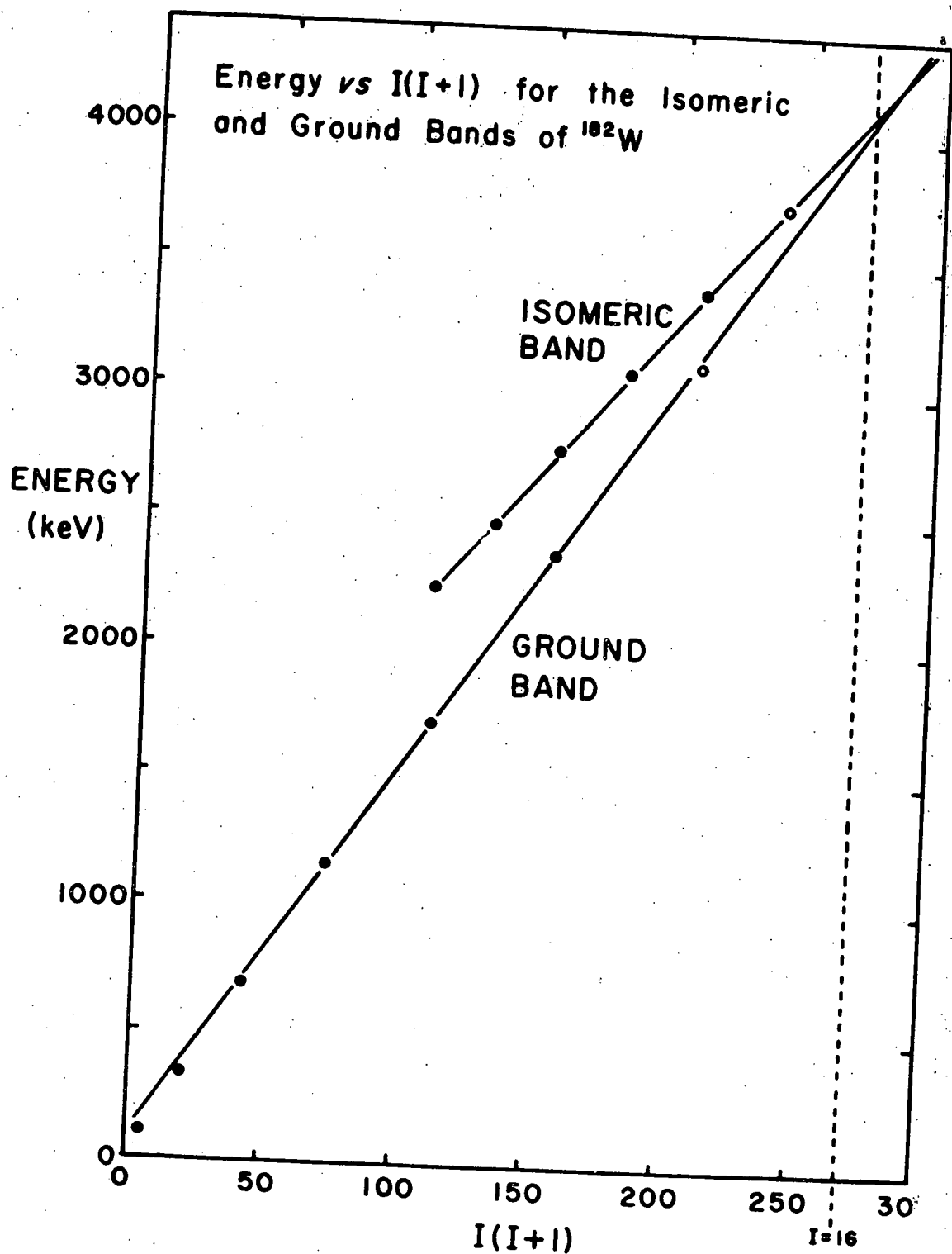


Figure 19. A plot of energy vs.  $I(I+1)$  for the ground and  $K^\pi = 10^+$  bands in  $^{102}\text{W}$

cannot be explored until a reaction can be done which transfers more angular momentum into the product nucleus. Such a reaction would be the  $^{182}\text{Hf}(\alpha, 4n)^{182}\text{W}$  reaction, which would populate higher spin states in  $^{182}\text{W}$  because of the higher incident beam energy. This reaction requires a target of  $^{182}\text{Hf}$ , which is unstable with a half-life of  $9 \times 10^6$  y, and which can only be produced in quantity by double neutron capture on  $^{180}\text{Hf}$ . An alternative method of populating high-spin states in  $^{182}\text{W}$  is by the  $^{176}\text{Yb}(^9\text{Be}, 3n)^{182}\text{W}$  reaction. However, the difficulties inherent in working with beryllium make such beams rare, so that this experiment was not feasible at this time.

The  $I^\pi = 0^+$  member of the  $\beta$  band was not seen in this work, and is taken from Kleinheinz [K173]. The vibrational states decay via  $E2$  transitions directly to the ground band [Sa70, Ga72]. These strong interband transitions are primarily a result of the energy dependence of  $E2$  transition probabilities, rather than mixing with the ground band. This conclusion is based on the fact that the  $I^\pi = 3^+$  and  $5^+$  members of the  $\gamma$ -band cannot be mixed with the ground band, but display decay properties similar to those of the  $\gamma$ -band states of even spin.

A plot of  $[E(I) - E(I-1)]/2I$  vs.  $2I^2$  (i.e. a "trumpet" plot) for the  $\gamma$ -band is shown in figure 20, and it is clear that the band is highly perturbed. In an attempt to account for the observed branching ratios and energy spacings, three-band-mixing calculations have been done by Günther *et al.* [Gu72] using unperturbed ground-,  $\beta$ -, and  $\gamma$ -band states as a basis set. However, these calculations did not include the  $4^+$  member of the  $\beta$  band or the  $5^+$  member of the  $\gamma$  band. Therefore, we

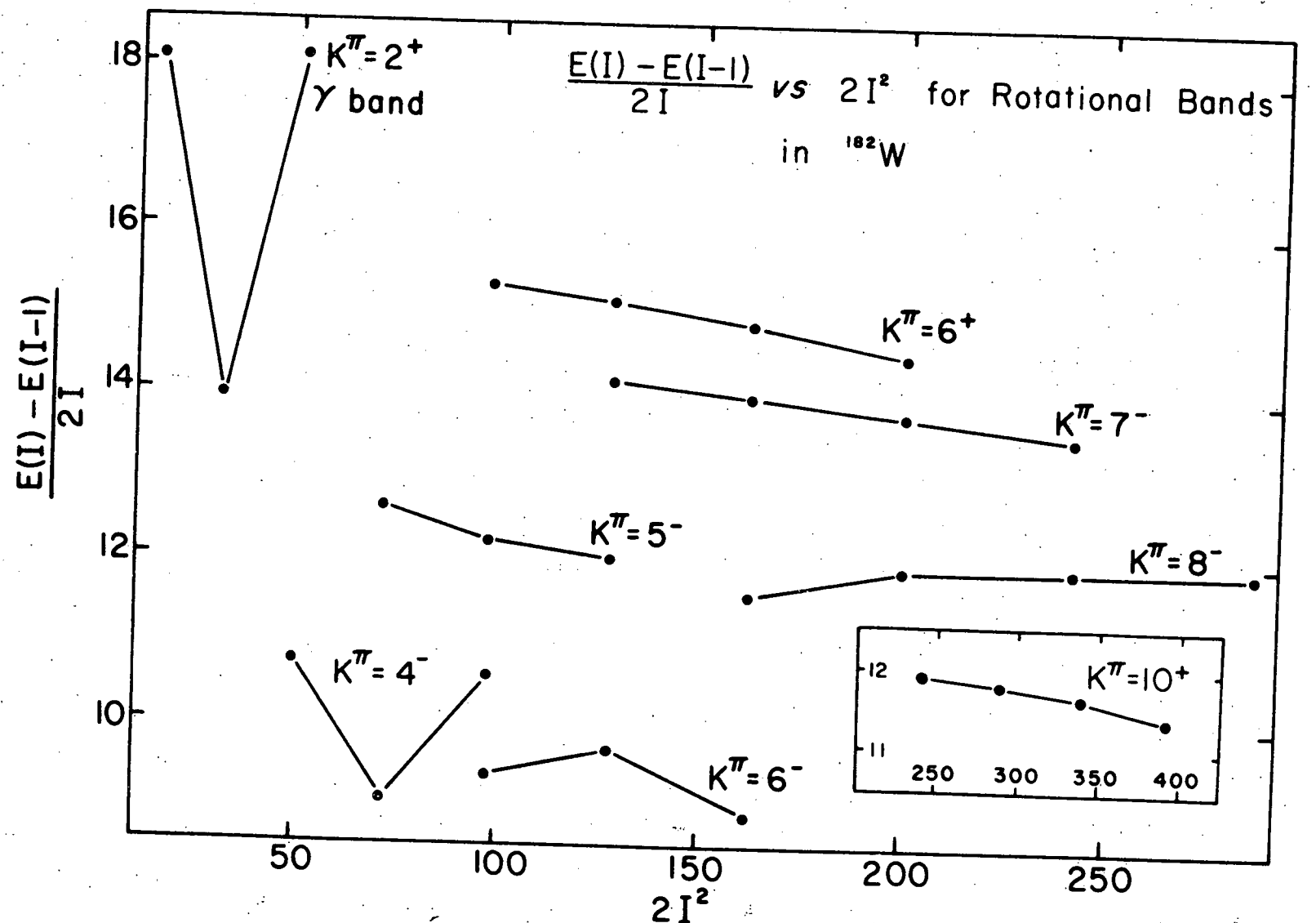


Figure 20.  $[E(I) - E(I-1)]/2I$  plotted vs.  $2I^2$  for some rotational bands observed in  $^{182}\text{W}$ .

have also done similar band mixing calculations in hopes of reproducing the energies of these states. The diagonal matrix elements are given by [Gu72]

$$E_K(I) = E_K + A_K[I(I+1) - K(K+1)] + B_K[I^2(I+1)^2 - K^2(K+1)^2] \quad (1)$$

while the off-diagonal elements are given by

$$\langle I, \gamma | H_{\text{coup}} | I, \text{GSB} \rangle = \sqrt{2(I-1)I(I+1)(I+2)} \langle \gamma | h^{\Delta K=2} | \text{GSB} \rangle$$

$$\langle I, \text{GSB} | H_{\text{coup}} | I, \beta \rangle = I(I+1) \langle \text{GSB} | h^{\Delta K=0} | \beta \rangle \quad (2)$$

$$\langle I, \beta | H_{\text{coup}} | I, \gamma \rangle = \sqrt{2(I-1)I(I+1)(I+2)} \langle \beta | h^{\Delta K=2} | \gamma \rangle$$

where the operators  $h^{\Delta K}$  are defined in refs. [Na64] and [Ma67]. In addition, Günther *et al.* uses the observed branching ratios from the  $K^{\pi}=2^-$  octupole band to the  $\beta$  and  $\gamma$  bands to determine the  $\beta$ - $\gamma$  interaction matrix element. Specifically, they note that the following equality

should hold:

$$\frac{B(E1, 2_{\text{oct}}^- \rightarrow 2_{\beta}^+)}{B(E1, 2_{\text{oct}}^- \rightarrow 2_{\gamma}^+)} = \frac{B(E1, 3_{\text{oct}}^- \rightarrow 2_{\beta}^+)}{B(E1, 3_{\text{oct}}^- \rightarrow 2_{\gamma}^+)} = (b/a)^2 \cong 0.15 \pm 0.01 \quad (3)$$

where  $(b/a)$  is the ratio of  $K = 2$  amplitude in the  $2^+$  state of the  $\beta$  and  $\gamma$  bands. These equalities assume that there is no  $K = 1$  amplitude admixed into the  $\beta$ ,  $\gamma$ , or octupole bands which would contribute to the  $B(E1)$  values, an assumption which is in fact not valid for the octupole band, as will be discussed in the section on the negative parity bands. Given the  $(b/a)^2$  ratio, Günther performed a two-band mixing calculation which yielded the interaction matrix element

$$|\langle \beta | h^{\Delta K=2} | \gamma \rangle| = 1.75 \pm 0.06 \text{ keV} \quad (4)$$

as well as the unperturbed energies of the  $\beta$  and  $\gamma$   $I^{\pi} = 2^+$  states, i.e.

$$E_{2^+}^{\beta} = 1252.7 \text{ keV} \quad (5)$$

$$E_{2^+}^{\gamma} = 1226.1 \text{ keV}$$

As a check on these calculations, note that the  $3^+$  and  $5^+$  members of the  $\gamma$  band remain unmixed within the framework of this calculation, so that the energies of these states may be used to determine the  $\gamma$ -band

rotational parameter and the  $\gamma$ -bandhead energy. For  $B_\gamma = 0$ , one obtains

$$E_{2+}^\gamma = 1233.6 \text{ keV} \quad (6)$$

and inclusion of any reasonable  $B$  term does not significantly affect this value because of the small value of  $I$ . It is clear that these two methods of determining the unperturbed  $\gamma$ -bandhead energy yield significantly different results, so that the value of  $|\langle \beta | h^{\Delta K=2} | \gamma \rangle|$  obtained by Günther *et al.* may be incorrect. As a result, we have treated this quantity as an adjustable parameter in our calculations. A list of all the parameters used in the calculations is given in Table 4, and the corresponding fits obtained using these parameters is given in Table 5. Fit I was obtained using the parameters given by Günther, and it is clear that the calculation fails to account for the energies of the highest experimentally observed  $\beta$  and  $\gamma$  states. In Fit II, the moment of inertia parameters of all three bands were constrained to have the same value, while in Fit III this parameter was forced to be identical only for the ground and  $\gamma$  bands. The fits were obtained using the computer code BETABLE [St68], which adjusts the input parameters such that the best least squares fit to the experimental energy spectrum is obtained. Accordingly, it is doubtful that a better fit to the data could be obtained without including additional adjustable parameters. Fit IV was obtained by matrix diagonalization using a rather arbitrary choice of input parameters, including a "B" term of 5 eV, and is included

TABLE 4  
Parameters Obtained in Three Band Mixing Calculations

Fit	$A_{GSB}$	$A_{\beta}$	$A_{\gamma}$	$B$ (eV)	$E_{GSB}^{0+}$	$E_{\beta}^{0+}$	$E_{\gamma}^{2+}$	$\langle G   h^{\Delta K=0}   \beta \rangle$	$\langle G   h^{\Delta K=1}   \beta \rangle$	$\langle \beta   h^{\Delta K=2}   \gamma \rangle$
I <sup>a</sup>	16.78	19.10	17.50	-5,0,0	0.0	1138	1226.1	-3.35	-0.62	1.75
II <sup>b</sup>	16.78	16.78	16.78	0,0,0	0.0	1137	1224.0	-3.73	1.55	1.37
III <sup>c</sup>	16.43	17.77	16.43	0,0,0	0.0	1137	1226.2	-1.50	1.60	1.17
IV <sup>d</sup>	16.8	16.8	16.8	-5,-5,-5	0.0	1138	1229.0	3.00	1.00	1.25

a) Parameters for this fit taken from reference 14.

b) Rotational parameters constrained to have the same value. In this fit  $B$ ,  $E_{GSB}^{0+}$  and  $E_{\beta}^{0+}$  were not allowed to vary.

c) Only GSB and  $\gamma$  rotational parameters constrained to have the same value.  $B$ ,  $E_{GSB}^{0+}$  and  $E_{\beta}^{0+}$  not allowed to vary.

d) No parameters were allowed to vary.

TABLE 5  
Results of 3-Band-mixing Fits

Fit	Deviation <sup>a)</sup> for GSB (keV)				Deviation <sup>a)</sup> for $\beta$ Band (keV)			Deviation <sup>a)</sup> for $\gamma$ Band (keV)				$6^+_{\gamma}$	$\Sigma  \Delta E $ <sup>b)</sup>
	$0^+$	$2^+$	$4^+$	$6^+$	$0^+$	$2^+$	$4^+$	$2^+$	$3^+$	$4^+$	$5^+$	Predicted	(keV)
I	0.0	0.0	0.3	-0.8	1.0	0.4	41.9	0.0	0.0	0.2	22.6	1790	67.2
II	0.0	0.0	-0.4	-5.6	0.0	-14.7	-6.2	-2.1	-6.6	3.1	3.1	1786	47.5
III <sup>c)</sup>	0.0	-1.7	-3.4	-2.1	0.0	-10.6	0.2	1.8	-6.4	-3.1	-3.1	1789	31.6
IV	0.0	0.2	0.9	0.3	1.0	-13.4	-5.4	2.5	-1.5	8.7	5.8	1760	39.7

a) Deviation =  $E_{\text{calc}} - E_{\text{expt.}}$

b)  $\Sigma |\Delta E|$  = sum of the absolute values of the deviations.

c) Allowing all three rotational parameters to vary did not significantly improve the fit. This would be expected, since in fit III a good fit could not be obtained for the  $\beta$  band even though  $A_{\beta}$  was allowed to vary independently.

to show that a definitive set of parameters cannot be determined on the basis of these calculations. In fact, it is clear from table 5 that, while a wide range of parameters give comparable fits to the data, no set of parameters gives a good fit. Specifically, the  $2^+$  member of the  $\beta$  band is much too low (or the  $4^+$  too high) in all of the calculations. Thus it would seem that the positive parity collective bands are not properly described by this model. There are a number of reasons why this might be the case. For instance, it may be that interactions other than those given by equations 2 exist between these states. In fact, it is well known that low-lying  $0^+$  states in this region tend not to be good vibrators, with ground and excited  $0^+$  states often strongly mixed [Be71]. Thus a thorough calculation would probably require more complex interactions. It is also possible that the failure of three-band-mixing to describe the collective states is due to an additional band, perhaps  $K = 1$  in character, mixing with these states. This possibility is strengthened by the failure of the octupole band branching ratios to determine correctly the  $K = 2$  amplitudes in the  $\beta$  and  $\gamma$  bands. As an example of how such mixing could occur, RPA calculations done by Hamamoto (quoted in [K173]) indicate that roughly 25% of the  $\gamma$  band is made up of the  $|K = 2, 3/2^-[512]\downarrow, 1/2^-[510]\uparrow\rangle$  state. This component can be Coriolis coupled directly with the  $|K = 1, 3/2^-[512]\downarrow, 1/2^-[510]\uparrow\rangle$  and  $|K = 1, 1/2^-[521]\downarrow, 1/2^-[510]\uparrow\rangle$  state, both of which have been tentatively assigned by Kleinheinz at approximately 2 MeV of excitation in  $^{182}\text{W}$  [K173].

In order to discuss the two-quasiparticle states in terms of the

Nilsson model, it is necessary to know in some detail the nuclear shape. It is especially important to know the value of the hexadecapole deformation  $\epsilon_4$  [Ni55], since this parameter has a strong influence on the level ordering [Be74b]. There has recently been some dispute concerning the value of this parameter in  $^{182}\text{W}$ . The hexadecapole transition moment for  $^{182}\text{W}$  has been deduced by Bemis *et al.* from a Coulomb excitation measurement with alpha particles [Bem73], and their results indicate a value for  $\epsilon_4$  of  $0.18 \pm 0.06$ , a factor of three greater than the value predicted by Nilsson *et al.* [Ni69]. This value is also substantially larger than that obtained by Hendrie ( $\epsilon_4 \cong 0.08$ ) from nuclear inelastic scattering on  $^{182}\text{W}$  [He73]. In an attempt to determine which value of  $\epsilon_4$  is most consistent with nuclear spectroscopic data, Coriolis band fitting calculations similar to those done for  $^{177}\text{Hf}$  were carried out for  $^{181}\text{W}$  [Be74b]. The results indicate that the best fit is obtained for values of  $\epsilon_4$  consistent with the predictions of Nilsson *et al.* [Ni69]. Therefore, the interpretation of the  $^{182}\text{W}$  level structure relies upon the Nilsson states corresponding to deformations of  $\epsilon_2 = 0.24$  and  $\epsilon_4 = 0.04$  (see figure 21). This value of  $\epsilon_4$  is slightly below Nilsson's prediction of  $\epsilon_4 = 0.065$ , but the difference is not enough to affect the qualitative arguments to be presented in the discussion of the two-quasiparticle states.

The  $K^\pi = 6^+$  two-quasi-proton band is rather unusual. The  $6^+$  assignment for the bandhead is taken from Galan *et al.* [Ga72], and the 214-keV transition from the 1971-keV state was found by Galan to be  $M1$ , in agreement with the assigned band structure. The intrinsic structure

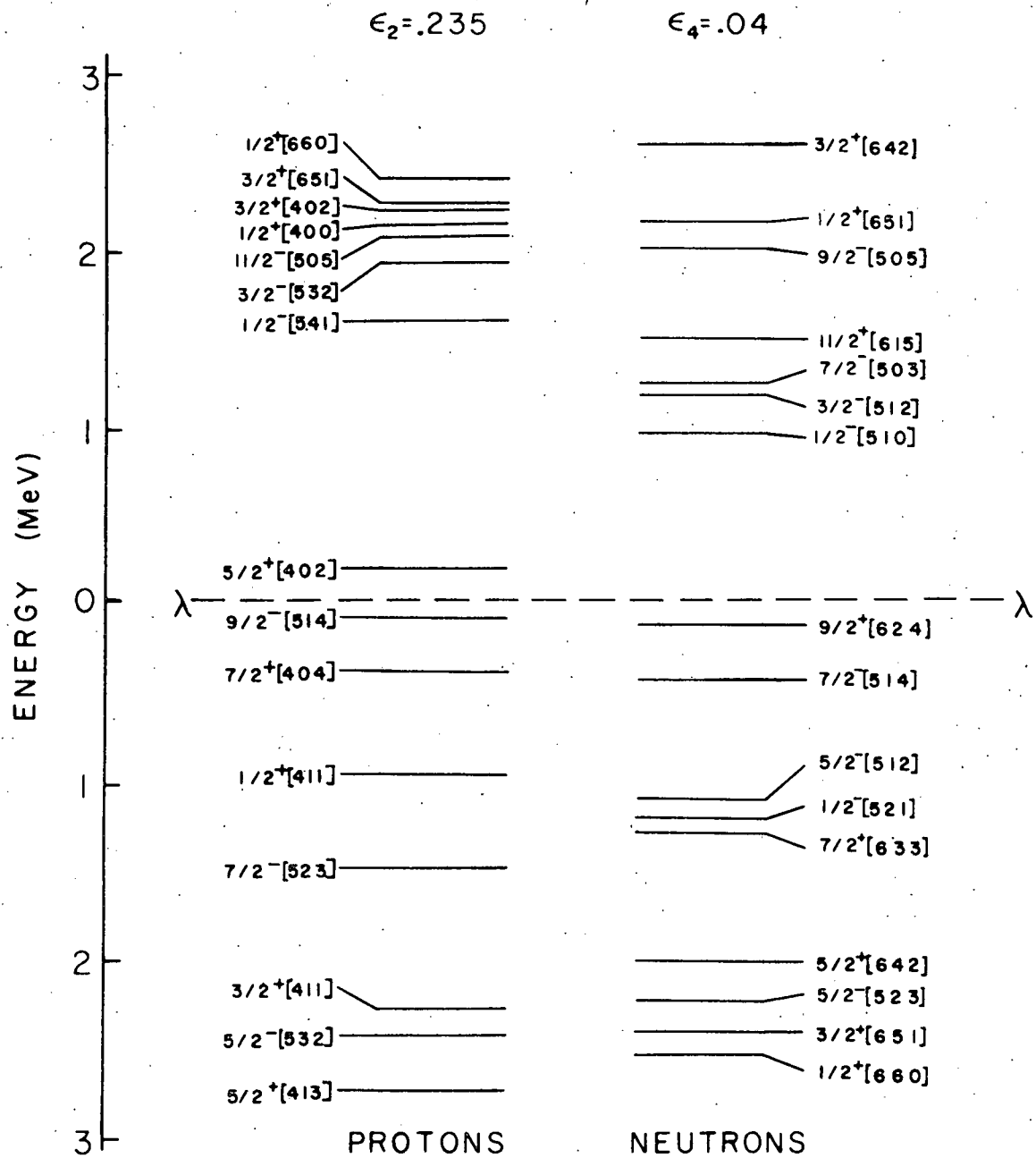


Figure 21. The diagram of Nilsson states for  $^{182}\text{W}$  assuming deformation parameters of  $\epsilon_2 = 0.235$  and  $\epsilon_4 = 0.04$ . The Fermi surface is placed arbitrarily just above the orbitals known to form the ground state in neighboring odd- $A$  nuclei. Level energies not corrected for pairing.

of the band is believed to be based on the singlet coupling of the  $5/2^+[402]$  and  $7/2^+[404]$  protons. The structure assignment is based on the observation that this band is seen in other even-even nuclei in this region [Kh73], and from the diagram of Nilsson states shown in figure 21, it can be seen that there is no other easy way to form a low-lying  $K^\pi = 6^+$  state. In addition, knowledge of the cascade-to-crossover ratios for  $\gamma$ -ray transitions within the band makes it possible to calculate, within the framework of the Nilsson model, the amplitudes of two-quasi-proton and two-quasi-neutron character present in the intrinsic particle structure of the band. Explicitly, the following equations may be developed [A164]:

$$1 + 1/\delta^2 = [(I+1)(I-1+K)(I-1-K)/2\lambda K^2(2I-1)] \cdot \{E(I \rightarrow I-2)/E(I \rightarrow I-1)\}^5 \quad (7)$$

where

$$\lambda = I_\gamma(I \rightarrow I-2)/I_\gamma(I \rightarrow I-1) \quad (8)$$

and

$$[|g_K - g_R|/Q_0] = [0.87\{E(I \rightarrow I-1)\}^2/(I^2-1)] \cdot (1/\delta^2) \quad (9)$$

where  $\delta$  is the  $E2/M1$  multipole mixing ratio for cascade transitions within the band,  $Q_0$  is the nuclear quadrupole moment, and  $g_R$  and  $g_K$  are respectively the rotational and intrinsic gyromagnetic ratios.

If one assumes that  $g_R$  for all rotational bands in  $^{182}\text{W}$  is the same, then a value for  $g_R$  can be taken from measurements of the g factor associated with the ground state rotational band [Gi67]. The quantity  $Q_0$  can be calculated from the  $B(E2)$  values obtained from Coulomb excitation studies through the relation [SG65]

$$Q_0 = [16B(E2)/5]^{1/2} \quad (10)$$

which holds explicitly only for the ground band, but which should apply reasonably well for the other rotational bands as well. Thus  $g_K$  can be deduced experimentally from the observed branching ratios. This value can then be compared with the theoretical value of  $g_K$  obtained from the Nilsson model. Specifically, in the asymptotic limit [Kh73],

$$g_K = (1/K)[g_s + g_\ell^{(K-1)}] \quad (11)$$

$$g_K = g_\ell$$

where  $g_s$  and  $g_\ell$  are the intrinsic and orbital g factors of the particle. Thus by comparison of the deduced and theoretical  $g_K$  values, it is often possible to make a statement about the neutron or proton character of the state. In the case of the  $K^\pi = 6^+$  band, the branching ratio for the spin 10 state at 2770.6 keV was determined and the results are given in table 6. The theoretical value of  $g_K$  for a singlet two-quasi-proton state is 1, which agrees with the average experimental

TABLE 6  
 $g_K$  from Branching Ratios for  $^{182}\text{W}$  Bands

$I^{\pi_K}$	Transition Energy	$I(\text{E}2)/I(\text{M}1)$	$ g_K - g_R /Q_0$ <sup>a)</sup>	$g_K$	Theoretical <sup>f)</sup> $g_K$	
					Singlet	Triplet
$10^+$ <sub>6</sub>	10 $\rightarrow$ 8 558.2	$0.57 \pm 0.3$ <sup>b)</sup>	$0.11 \pm 0.03$	$0.96 \pm 0.19$	1	1.39 Protons
	10 $\rightarrow$ 9 290.4			$-0.46 \pm 0.19$	0	-0.34 Neutrons
$10^+$ <sub>6</sub>	10 $\rightarrow$ 8 558.2	$0.48 \pm 0.3$ <sup>c)</sup>	$0.12 \pm 0.04$	$1.02 \pm 0.26$	1	1.39 Protons
	10 $\rightarrow$ 9 290.4			$-0.53 \pm 0.26$	0	-0.34 Neutrons
$13^+$ <sub>10</sub>	13 $\rightarrow$ 12 586.0	$0.2 \pm 0.1$ <sup>d)</sup>	$0.081 \pm 0.020$	$0.77 \pm 0.13$ <sup>e)</sup>	1	1.25 Protons
	13 $\rightarrow$ 11 302.0			$-0.27 \pm 0.13$	0	-0.23 Neutrons

a) The value for  $Q_0$  is taken from SG65.

The value for  $g_R$  is taken from Gi67.

b) This branching ratio taken from singles. Large error results from uncertainty in resolving the weak doublet at 557 keV.

c) This value taken from the 241.6-keV coincidence gate. Large uncertainty results from angular correlation effects and uncertainty in the relative efficiency for detecting these  $\gamma$ -rays.

TABLE 6 - FOOTNOTES (Contd.)

- d) This value could only be obtained from coincidence data (262.3 keV gate) as the 58.6-keV  $\gamma$ -ray is believed to be the smaller component of an unresolved doublet.
- e) For 100% error in  $I(E2)/I(M1)$ , error in  $g_K = \pm 0.26$ .
- f) cf. equations 11. The value of  $g_s$  used in this calculation is the so called quenched value, obtained somewhat arbitrarily by using a value which is 60% that for a nucleon in free space.

value of  $0.99 \pm 0.16$ . There is, however, a piece of evidence which argues strongly against this band being  $K = 6$  in character, i.e. the bandhead decays promptly to the  $K = 0$  ground band. In  $^{176}\text{Hf}$ , on the other hand, the  $K^\pi = 6^+$  two-quasiparticle bandhead at 1333.1 keV decays with a half-life of almost 10  $\mu\text{s}$  [Kh73]. While it is true that  $K$  is not generally a good quantum number in this region, the plot of  $[\text{E}(\text{I}) - \text{E}(\text{I}-1)]/2\text{I}$  vs.  $2\text{I}^2$  (figure 20) gives little indication that this band is strongly mixed, as the points are nearly linear and do not indicate the compression expected for a strongly mixed band (note for instance the points associated with the  $K^\pi = 4^-$ ,  $5^-$ , or  $6^-$  bands). Since the  $K^\pi = 6^+$  band does not seem to be strongly mixed, the  $K$ -forbidden  $\gamma$ -ray transitions out of the 1756.8-keV state should be highly hindered, and a measurable lifetime for the state is expected.

A possible explanation of this behavior lies in a rather unusual mixing with the  $\gamma$  band. To the best of our knowledge, this mixing has not been observed in other nuclei where both bands are present. However, the probable near-degeneracy of the two  $6^+$  states in  $^{182}\text{W}$  may cause some mixing to occur. While the  $6^+$  member of the  $\gamma$  band was not seen experimentally, it is apparent from the level scheme that the two  $6^+$  states are within at least 50 keV of each other, and it was hoped that the three-band-mixing calculations would yield an accurate estimate of the energy of the  $\text{I}^\pi \text{K} = 6^+ 2$  state. Though a reliable prediction could not be obtained, it is clear from table 5 that the two  $6^+$  states are probably within 30 keV of each other, and if a significant "B" term is present (as would be expected), they may well lie within 10 keV.

Because of this near degeneracy, only a small interaction need be present to result in mixing sufficient to lead to prompt decay of the  $K^\pi = 6^+$  bandhead. Since the half-life of the  $\gamma$  bandhead is known from Coulomb excitation studies [Alc58] to be roughly 0.3 ps, only about 0.01%  $\gamma$ -band admixture need be present in the  $K = 6$  band to put the half-life below our experimental lower limit. Weaker evidence that the prompt decay of the  $K^\pi = 6^+$  bandhead results from mixing with the  $\gamma$  band is given in table 7, in which the  $B(E2)$  ratios for  $\gamma$ -ray transitions from the states of interest to the ground band are compared with the theoretical values [Ala55] given by

$$\frac{B(E2, IK \rightarrow I' K')}{B(E2, IK \rightarrow I'' K'')} = \left| \langle I \lambda K \Delta K | I' K' \rangle \right|^2 \quad (12)$$

where the  $\langle I \lambda K \Delta K | I' K' \rangle$  are the appropriate Clebsch-Gordan coefficients. It is seen that the  $\gamma$ -band transitions systematically populate the higher-spin member of the ground band more strongly than predicted by theory. The theoretical value quoted for the  $K = 6$  band is calculated assuming that the entire transition strength is a result of  $K = 2$  admixture, and again the theoretical value is less than the experimental value, as is the case for decays from the  $\gamma$  band. Therefore the assignment of the 1756.8-keV band as being predominantly  $K^\pi = 6^+$  is believed to be correct, and the short half-life of the  $K^\pi = 6^+$  state is due to mixing with the  $6^+$  member of the  $\gamma$  band.

The remaining positive parity band seen in this study is that

TABLE 7

Comparison of Experimental B(E2) Ratios with Alaga

Rules for the  $\gamma$  and  $K^\pi = 6^+$  Bands

Transitions (IK→I'K')	Experimental <sup>a)</sup> B(E2) Ratio	Alaga Rules	% Deviation <sup>b)</sup>
(22→20)/(22→00)	2.0 ±0.2	1.43	+40%
(32→40)/(32→20)	0.55±0.6	0.400	+40%
(42→40)/(42→20)	4.6 ±0.5	2.95	+60%
(52→60)/(52→40)	0.62±0.3	0.571	+ 9%
(66→60)/(66→40)	4.8 ±0.5	3.71 <sup>c)</sup>	+29%

a) Note that the ratio is such that the B(E2) value corresponding to decay to the higher spin member is the numerator.

b) Deviation is defined here as  $(\text{experimental-Alaga rules}) / (\text{Alaga rules})$ .

c) The theoretical value was obtained by assuming that all the transition strength is due to  $K = 2$  admixture in the  $K = 6$  band. For  $K = 1$ , Alaga rules predict the ratio to be 0.037.

based on the isomeric state at 2230 keV. Nordhagen *et al.* [No71] found this state to have a half-life of 1.4  $\mu$ s and assigned that state a spin and parity of  $I^\pi = 9^+$  or  $10^+$ . From the diagram of Nilsson states (figure 21), it can be seen that a low-lying  $K^\pi = 10^+$  state could be formed by a triplet coupling of the  $9/2^-$ [514] and  $11/2^-$ [505] protons or the  $9/2^+$ [624] and  $11/2^+$ [615] neutrons. On the other hand, low-lying  $9^+$  states are difficult to construct, so that the  $K^\pi = 10^+$  assignment is preferred. Since either protons or neutrons may couple to form this state, it was desirable to identify the band members based on the two-quasiparticle state so that the branching ratios could be used to determine the intrinsic character of the state by evaluation of  $g_K$ . Because this state is isomeric, the  $\gamma$  rays associated with the intraband transitions could not be seen in prompt coincidence with the isomeric or ground band transitions. However, by setting a gate off the prompt TAC peak, delayed coincidences could be seen. The prompt and delayed coincidence spectra for the 518.5-keV gate are shown in figure 22. The 262- and 283-keV  $\gamma$  rays are present in the delayed spectrum, and prompt coincidence gates set on these  $\gamma$  rays (figure 23) allow the  $K^\pi = 10^+$  band members to be identified with reasonable confidence up to  $I = 14$ , and tentatively up to  $I = 15$ . From the 262-keV coincidence gate, the branching ratio from the 3077.1-keV state was determined for the band. The theoretical value of  $g_K$  for triplet protons is 1.25, and for triplet neutrons is -0.23 (cf. equations 11), and from table 6 (cf. footnote e) it is seen that, even if the intensity of the 586-keV transition were in error by 100%, the

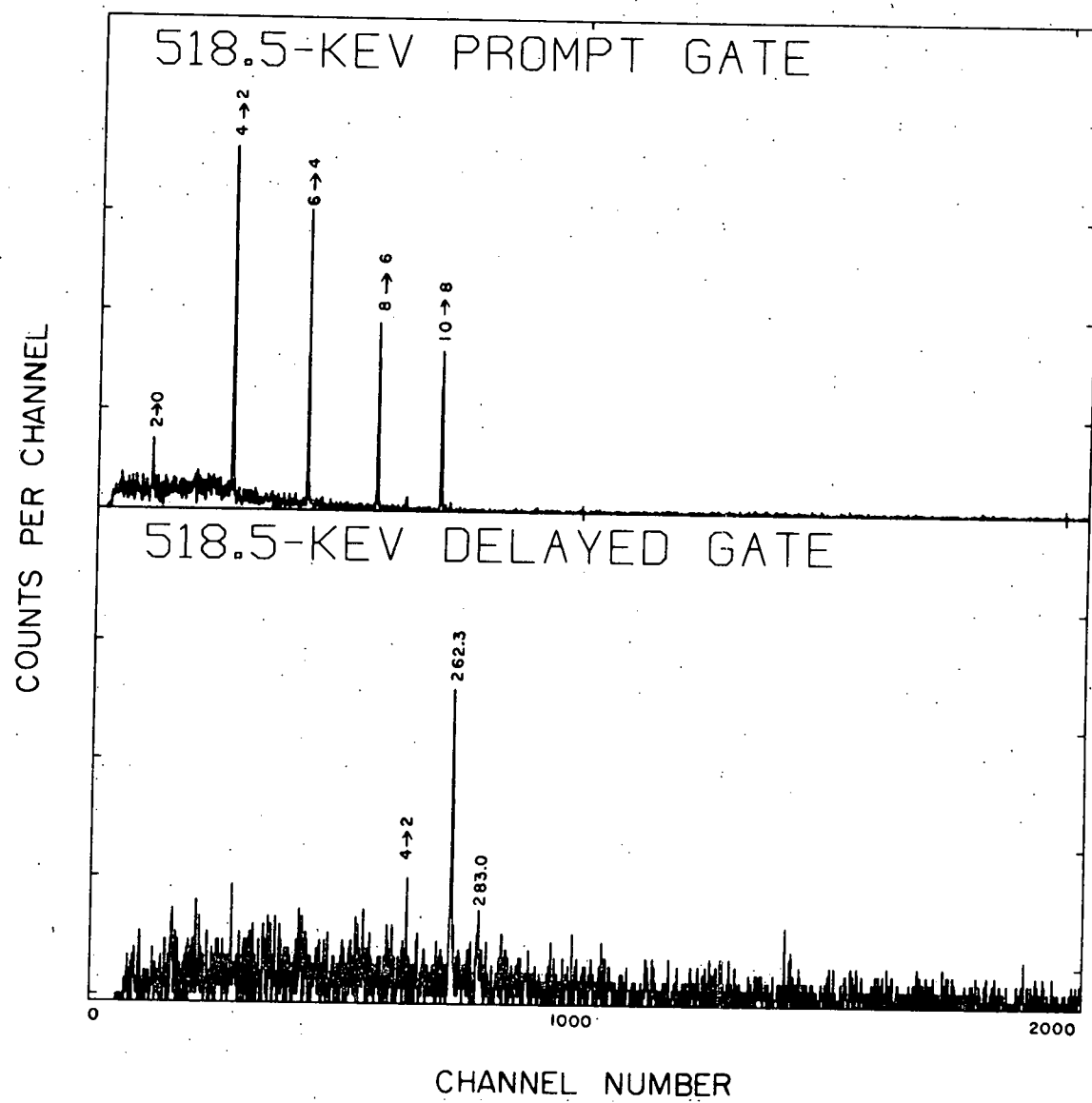


Figure 22. The prompt and delayed coincidence spectra for the 518.5-keV gated transition.

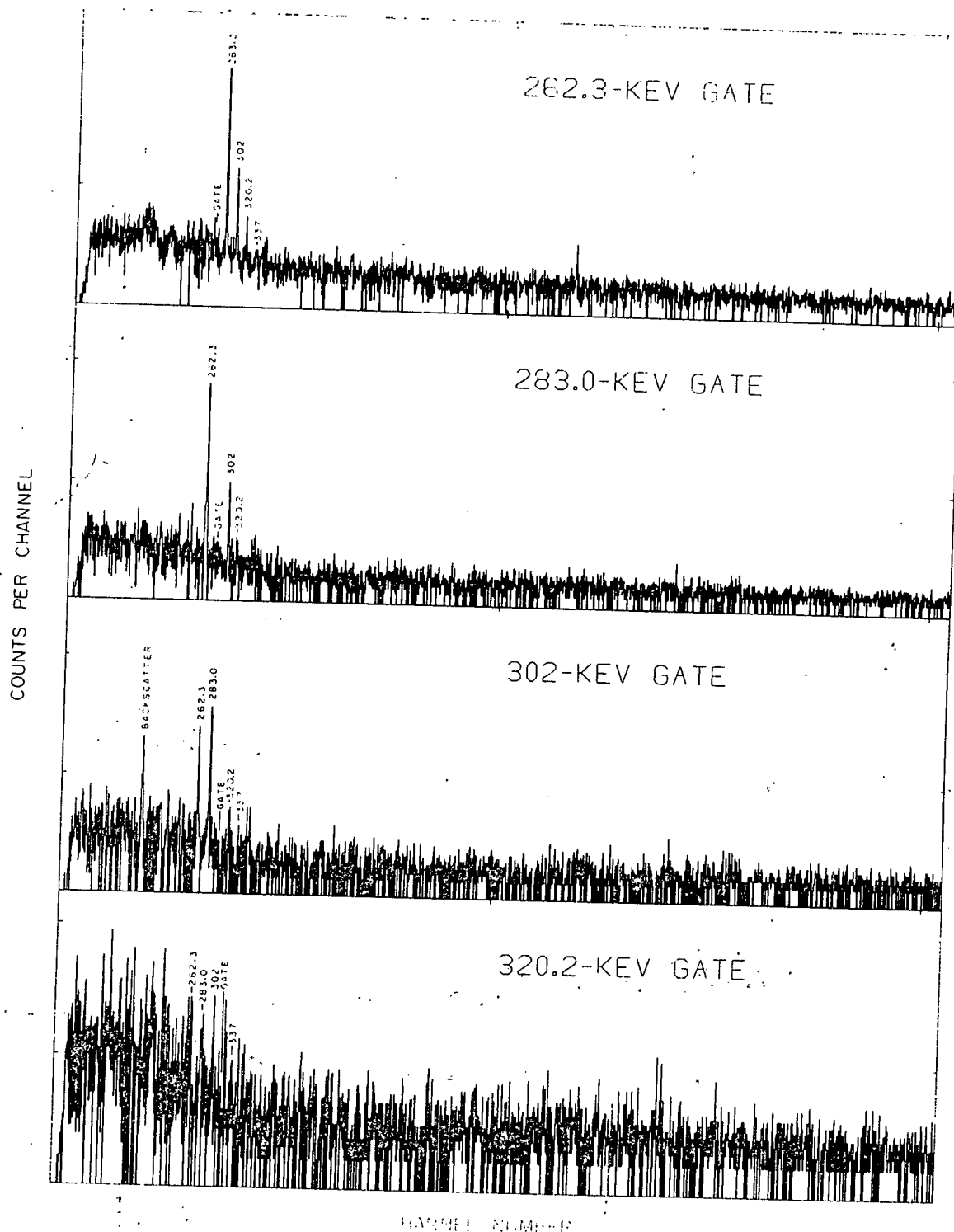


Figure 23. The prompt coincidence spectra associated with the  $K^\pi = 10^+$  isomeric band.

branching ratio would still indicate that this high-K band was a two-quasi-neutron band. Thus we assign this band as based on the  $|9/2^+[624\uparrow], 11/2^+[615\uparrow]\rangle$  state.

The measured half-life of 1.4  $\mu$ s for the  $K = 10$  isomer is actually much less than one might have expected. To see this, we calculate the retardation factor  $F_W$ , defined by

$$F_W = T_{1/2}(\text{expt})/T_{1/2}(\text{SP}) \quad (13)$$

where  $T_{1/2}(\text{SP})$  is the half-life calculated from the Moszkowski single particle estimate, given for  $E2$  transitions by [Mo55]

$$T_{1/2}(\text{SP}) = \ln 2 / [1.6 \times 10^8 A^{4/3} E_Y^5] \quad (14)$$

In the case of the 1.4  $\mu$ s isomer, one obtains

$$F_W = 5.2 \times 10^5 \quad (15)$$

and since the transitions are eight orders K-forbidden it follows that the decays are hindered by a factor of 5.2 per degree of K-forbiddenness. However, it is generally found experimentally that decays are hindered by a factor of 10 to 100 per degree of K-forbiddenness in deformed nuclei. Thus, if the  $K = 10$  state had been hindered by  $10^8$ , its half-life would have been  $\approx 300 \mu$ s. The relatively small retardation

factor for the  $K = 10$  bandhead implies that  $K$  is a poor quantum number for the band. This would be expected from the plot of  $[E(I)-E(I-1)]/2I$  vs.  $2I^2$  for the band (figure 20), where it is seen that the band-member spacings are somewhat compressed relative to the nearly pure proton bands.

## 2. Odd Parity Bands

The  $K^\pi = 2^-$  band was seen up to spin 4 in the transfer reaction work of Kleinheinz *et al.* [K173], and much evidence has accumulated indicating that the band is based on an octupole vibration [Gü72, K173, He72]. In  $\beta$ -decay studies, the band was established to  $I = 6$  [Sa70], and in-beam it is excited to  $I = 11$  (see figure 24). The higher band assignments are based on the energy spacings of the levels and the observed increase of cascade-to-crossover  $\gamma$ -ray intensity as angular momentum increases, a result of the  $E^5$  dependence of the  $E2$  transition probability.

As indicated by the trumpet plot of figure 25, the octupole band is strongly perturbed; the points form two branches with the odd spin members depressed. These odd-even shifts arise from second order Coriolis mixing with the  $K = 0$  octupole band through the  $K = 1$  octupole band [Kh73b]. Only odd-spin members of the  $K = 0$  band are expected to lie at low energy, so that only the odd-spin members of the  $K = 2$  band are expected to be significantly mixed. As the locations of the  $K = 0$  and  $K = 1$  octupole bands are not known, an experimental estimate of the interaction matrix elements cannot be made, although

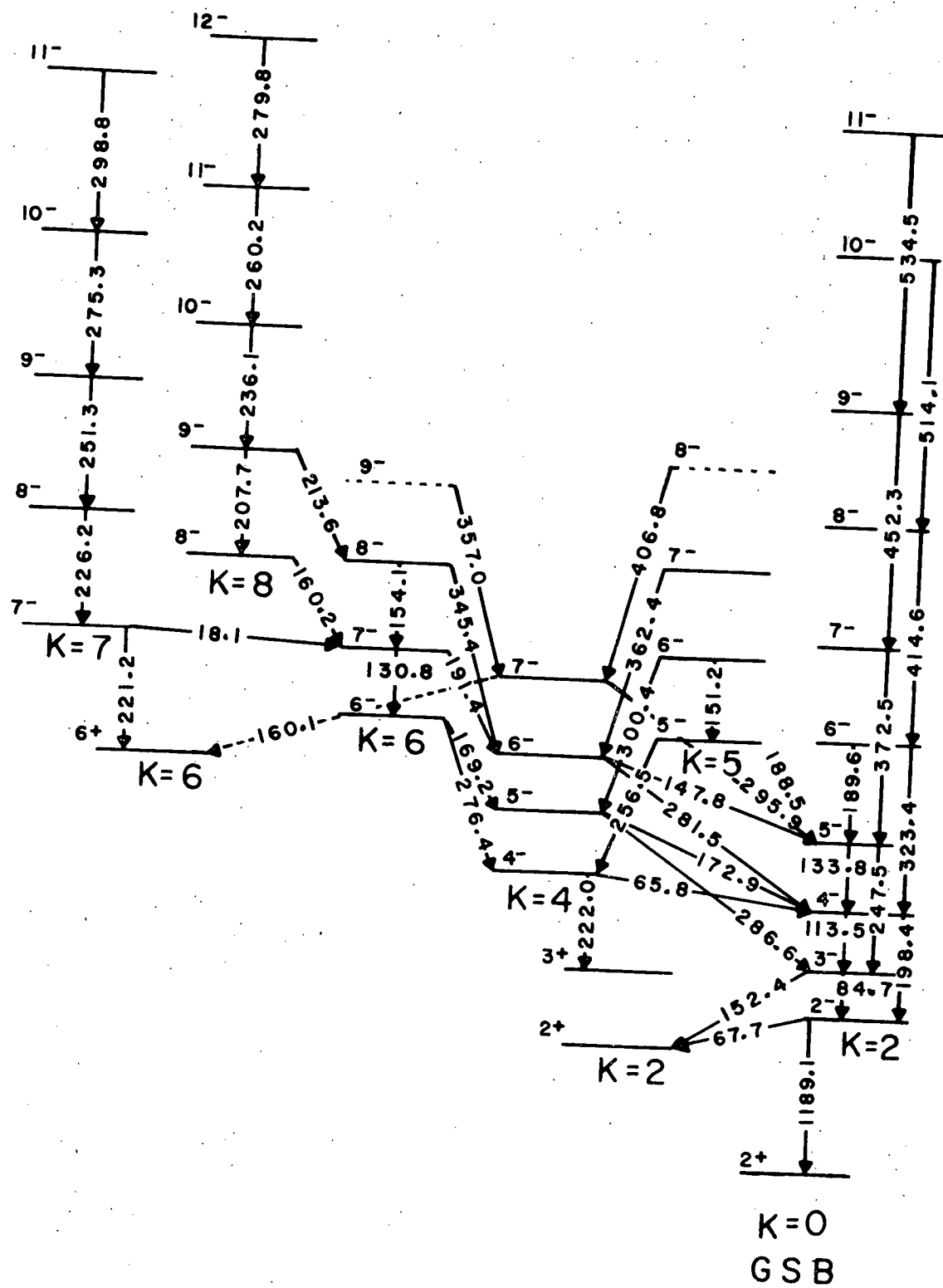


Figure 24. The odd parity band structure observed in  $^{182}\text{W}$ . Only the two most intense transitions associated with each level are shown. Refer to figure 13 for level energies.

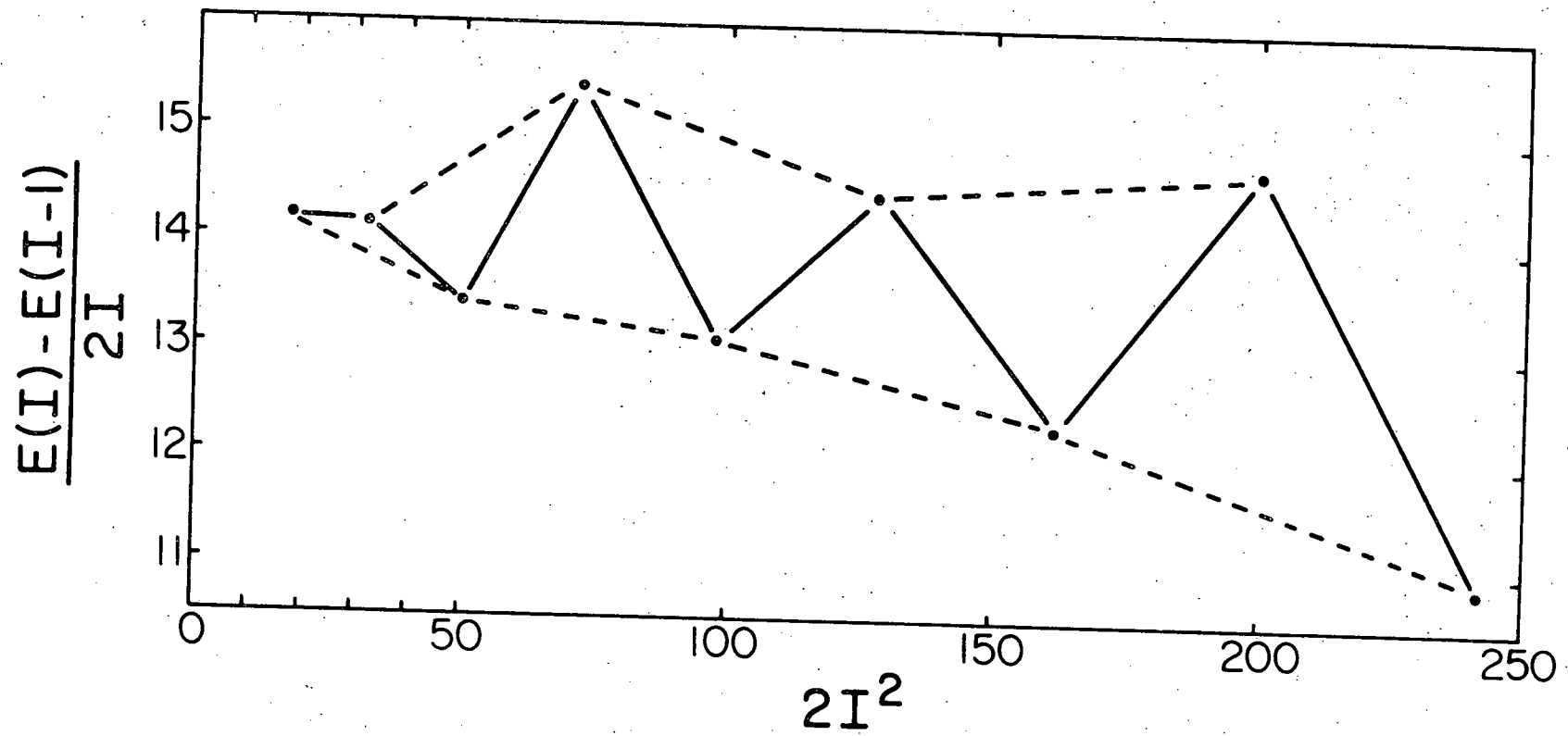


Figure 25.  $[E(I) - E(I-1)]/2I$  plotted vs.  $2I^2$  for the  $K^{\pi} = 2^-$  octupole bands in  $^{182}\text{W}$ .

theoretical matrix elements and bandhead energies have been calculated by Neergård and Vogel [Ne70]. Several papers exist in the literature dealing with the properties of the octupole band [He72, GU72], and the calculations done in these works were carried out under the assumption that no  $K = 0$  or  $K = 1$  admixture is present in the  $K = 2$  band. The large perturbations shown by the  $[E(I)-E(I-1)]/2I$  vs.  $2I^2$  plot place this assumption in question for the high-spin members of the band. For the low spin states, however, the assumption is probably reasonable.

Note that the upper branch of the octupole band trumpet plot shows a marked deviation from smooth behavior for the point representing the energy difference between the  $I = 6$  and  $I = 5$  states. This anomalous point is the result of mixing with the  $K^T = 4^-$  band. Because the  $I = 5$  and  $I = 6$  states of the  $K = 4$  band both lie between the  $I = 5$  and  $I = 6$  states of the octupole band, the octupole states tend to be pushed apart. In contrast, the two  $K = 4$  states tend to be pushed together, as can be seen on the trumpet plot for this band (figure 20). The strong mixing of the  $K = 4$  band with the octupole band is also implied by the fact that the  $K = 4$  states decay primarily to the octupole states rather than via intraband cascades.

The  $K^T = 4^-$ ,  $5^-$ , and  $6^-$  bands were all seen in the  $(d, t)$  and  $(\tau, \alpha)$  reaction work of Kleinheinz *et al.* [K173], and the Nilsson assignments shown in figure 13 are taken from that work. The highest state in the  $K = 5$  band and the highest two states in the  $K = 6$  band were seen only in this work and are assigned to these bands solely on the basis of

energy spacings and decay patterns. The transfer reaction studies indicated that these three bands were strongly mixed, and the interband transition strength seen here supports this.

The remaining two negative parity bands are given tentative Nilsson and spin assignments on the basis of somewhat meager evidence. The bandhead at 1978 keV (figure 13) is known to be  $I^\pi = 6^-$  or  $7^-$  from the decay studies [Sa70, Ga72], but the intense 18-keV decay to the  $7^-$  state at 1960 keV (figure 24) implies that these two states may be highly mixed, lending support to the  $K^\pi = 7^-$  assignment. As the  $|9/2^-[514\uparrow], 5/2^+[402\uparrow]\rangle$  two-quasi-proton state is expected to lie quite low in the spectrum, this assignment is preferred, although other reasonably low-lying neutron and proton  $I^\pi = 7^-$  two-quasiparticle states can be formed. It seems probable, however, that the band is based on a two-quasi-proton state, since the 1978-keV state decays via a strong 221-keV  $\gamma$  ray to the  $K^\pi = 6^+$  two-quasi-proton bandhead. Since these bands are of different parity, no mixing can occur between them. As a result, if the  $K^\pi = 7^-$  band were a two-quasi-neutron band, decay to the  $K^\pi = 6^+$  bandhead should be quite hindered compared to decays to the two-quasi-neutron states. Thus, the presence of the relatively strong 221-keV transition implies that the  $K^\pi = 7^-$  band is a proton band.

If the conclusions of the preceding discussion are correct, then the mixing between the 1978- and 1960-keV states is an example of neutron-proton mixing. It should be noted that if this is true, the

mixing results from the near degeneracy of the two states. This is an important point to keep in mind, as the two states do not satisfy the conditions usually required for significant configuration mixing [Ma74]. It has generally been observed experimentally that  $\Delta K = 0$  for two bands which are mixed through the neutron-proton residual interaction. Of course  $K$  is not strictly a good quantum number, so that the configuration mixing might be taking place through states which are Coriolis mixed with the  $K = 6$  or  $7$  bands. However, these neutron-proton mixings would violate the experimentally observed tendency of significant configuration mixing occurring only when the unpaired particles occupy orbitals on both sides of the Fermi surface. That this should be necessary can be seen by looking at the form of the off diagonal matrix element  $m$  for the interaction [Ma74], i.e.

$$m = \langle \psi_{n_1 n_2} | V^{N-P} | \psi_{p_1 p_2} \rangle \quad (16)$$

where  $|\psi_{n_1 n_2}\rangle$  is the two-quasi-neutron excited state, and  $V^{N-P}$  is the residual interaction. In the second quantization formalism,  $V^{N-P}$  can be written as

$$V^{N-P} = \sum_{npn'p'} \langle np | V_{np} | n' p' \rangle a_n^+ a_p^+ a_{n'} a_{p'} \quad (17)$$

where  $a$  and  $a^+$  are the nucleon annihilation and creation operators.

For the case of parallel couplings of the proton and neutron angular

momentum, the off diagonal matrix element becomes [Ma74]

$$|m| = |(u_{n_1} v_{n_2} u_{p_1} v_{p_2} + v_{n_1} u_{n_2} v_{p_1} u_{p_2}) \langle n_1 \bar{p}_2 | v_{np} | \bar{n}_2 p_1 \rangle - (u_{n_1} v_{n_2} v_{p_1} u_{p_2} + v_{n_1} u_{n_2} u_{p_1} v_{p_2}) \langle n_1 \bar{p}_1 | v_{np} | \bar{n}_2 p_2 \rangle| \quad (18)$$

where  $u$  and  $v$  are the usual occupation numbers defined in the BCS treatment of the pairing interaction [Be159]. The important point to notice is that in the pairing factors of equation 18, only the combination  $uv$  occurs. Because  $u$  is large for orbitals above and  $v$  for orbitals below the Fermi surface, the product, and thus the off-diagonal matrix element, is largest when the orbitals of interest straddle the Fermi surface. In the case of the 1978- and 1960-keV states, it can be seen from the Nilsson diagram of figure 21 that neutron-proton mixing between low-lying components of the same  $K$  would violate this condition. However, the nearly degenerate energies of these two states could cause appreciable mixing even for a small interaction, so that this interpretation is still reasonable.

The remaining band seen in this work is the very tentative  $K^\pi = 8^-$  band. An interesting characteristic of this band is the sudden appearance of a strong interband transition out of the 2328-keV state. This branching can be understood if the 2120.2-keV state were  $I^\pi = 8^-$  and it were mixed with the  $I^\pi = 8^-$  state of the  $K^\pi = 6^-$  band at 2114.1 keV. Since the perturbed energies are only 6 keV apart, an interaction matrix element of only 3 keV (in the approximation of two-band mixing)

would account for the splitting if the states were initially degenerate, and Coriolis interactions could easily account for a matrix element of this magnitude. The perturbations implied by the trumpet plots for these bands are also consistent with mixing between these states. And finally, from the Nilsson states shown in figure 21, one would expect the  $K^\pi = 8^-$  band to lie slightly below the  $K^\pi = 10^+$  isomeric band, as this band does. On the basis of these arguments, the band is tentatively assigned to be a two-quasi-neutron band formed by the triplet coupling of the  $9/2^+[624]$  and  $7/2^-[503]$  neutrons.

#### E. SUMMARY AND CONCLUSIONS

As a result of the presence of a large number of low-lying high- $K$  bands in  $^{182}\text{W}$ , the in-beam investigation produced considerable new information for high-lying members of an unusually large number of rotational bands. The apparent success of the Nilsson model in predicting the observed two-quasiparticle states for the deformation parameters  $\epsilon_2 = 0.24$  and  $\epsilon_4 = 0.04-0.06$  indicates that the spectroscopic information supports the nuclear deformation predicted by Nilsson, and argues strongly that the deformed shell model gives at least qualitatively an accurate description of nuclear structure in this region of the periodic table.

Because of the current interest in backbending and the experimental identification of the  $K = 10$  two-quasi-neutron band, it would be of interest to examine higher spin states in  $^{182}\text{W}$ . If the  $K = 10$  band were to become sufficiently decoupled at higher spins, backbending

behavior could appear in the *yrast* band and would be proof that the  $i_{13/2}$  neutron band crossing model of Stephens and Simon is qualitatively correct, at least in some cases. Thus the  $^{176}\text{Yb}(^9\text{Be}, 3n)^{182}\text{W}$  reaction would be a very interesting reaction to study. It would also be of interest to determine whether the  $K = 10$  isomer occurs in  $^{184}\text{Os}$ , an isotope of  $^{182}\text{W}$ . This nucleus apparently does display backbending in the ground band [Wa73], and it is conceivable that the " $K^\pi = 10^+$ " band is responsible for the behavior, though a band structured from a more conventional Stephens-Simon type recoupling of the two  $i_{13/2}$  neutrons nearest the Fermi surface may also be present near the " $K = 10$ " band in  $^{184}\text{Os}$ .

In conclusion, it is clear that many more data for high spin states will be needed before the collective and intrinsic structure of such states can be completely understood. The relatively large number of collective and high- $K$  two-quasiparticle bands observed for  $^{182}\text{W}$  should be a valuable aid in achieving this understanding.

IV. THE DECAY OF  $^{182m}\text{Re}$  TO  $^{182}\text{W}$ 

The decay of  $^{182m}\text{Re}$  was investigated principally because the in-beam  $\gamma$ -ray spectroscopy study indicated that errors existed in the current decay scheme [Sa70, Ga72]. The principal tool used in this study was the two-parameter  $\gamma$ - $\gamma$  coincidence technique. In addition, the high-resolution singles spectrum shown in figure 26 was collected so that  $\gamma$ -ray energies and intensities in the complex low-energy region of the spectrum could be measured accurately.

The  $^{182m}\text{Re}$  activity was produced by bombarding a 1-mil natural tantalum foil with a 41-MeV beam of alpha particles produced by the MSU cyclotron. The source was allowed to cool for four days to eliminate  $^{13}\text{h}^{182g}\text{Re}$ . Coincidence data were taken at  $90^\circ$  geometry with detectors of 18% and 10% efficiency. Table 8 lists the  $\gamma$ -rays placed in the  $^{182m}\text{Re}$  decay scheme, which is shown in figure 27. Some coincidence gates associated with this decay are shown in figure 28. Figure 28a shows the 226.2-keV gate, and it is seen that the 221.6-keV  $\gamma$ -ray is the most prominent line in the spectrum, indicating that the 226.2-keV  $\gamma$ -ray is a transition to the 1978.4-keV level. The presence in this spectrum of  $\gamma$ -rays associated with the 1960.3-keV level requires the existence of the intense 18-keV transition seen by [Ha61] from the 1978.4-keV level. Figures 28b and 28c show the spectra associated with gates set on the high- and low-energy portions of the 300-keV doublet. It is apparent that the gates are very similar, and

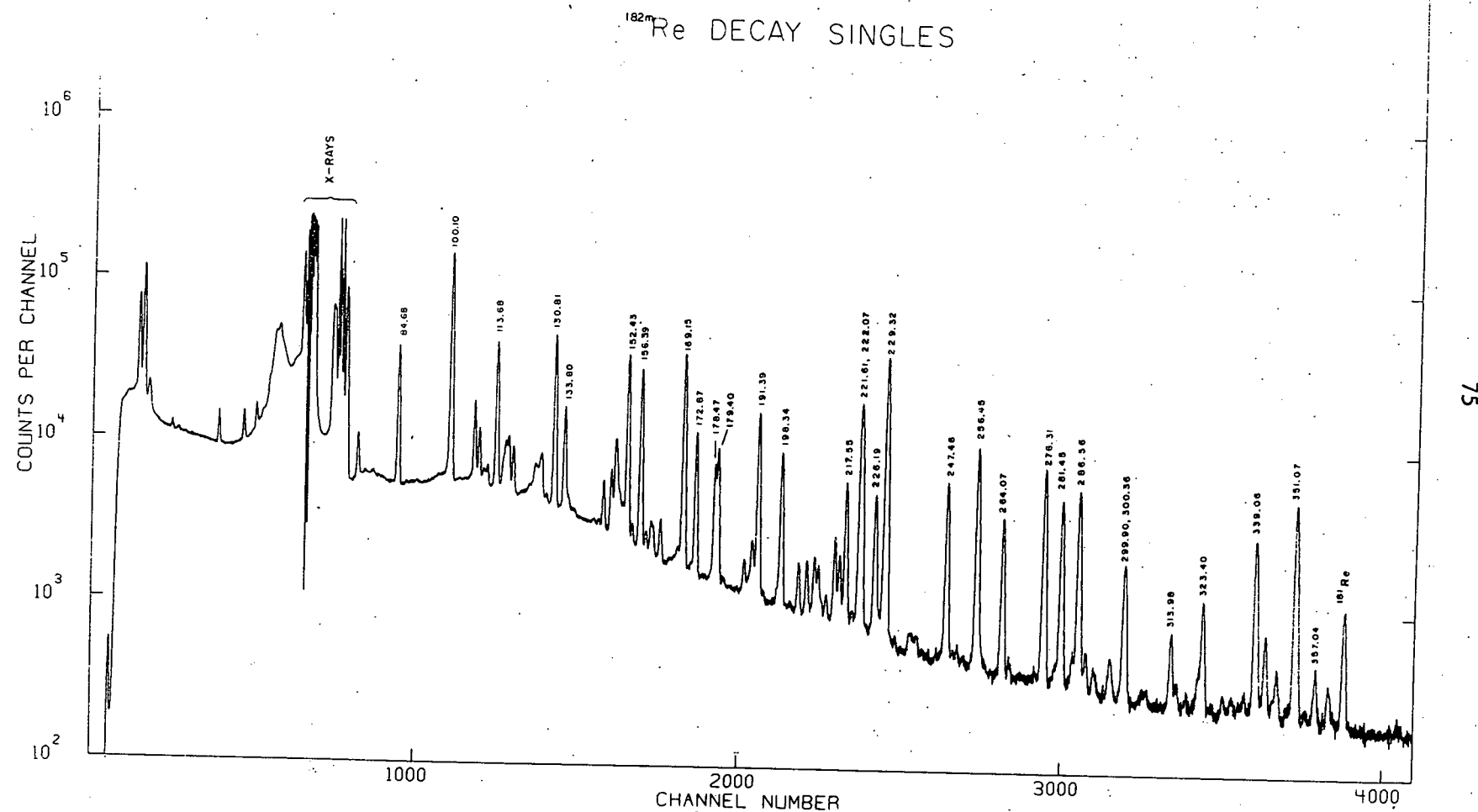


Figure 26. The high-resolution  $\gamma$ -ray singles spectrum associated with the decay of 64 hr <sup>182m</sup>Re.

TABLE 8

 $\gamma$ -Rays Associated with the Decay of  $^{182m}\text{Re}$ 

Energy <sup>a)</sup>	$\gamma$ -ray Intensity <sup>b)</sup>	Energy <sup>a)</sup>	$\gamma$ -ray Intensity <sup>b)</sup>
18.05	-	160.1	9.3 (0.6)
19.85	-	169.15	440 (30)
31.7	34 (16)	172.87	139 (9)
39.1	12 (3)	178.47	88 (5)
42.7	11 (1)	179.40	117 (7)
60.65	4 (2)	187.34	12.5 (1.2)
65.8	106 (10)	188.54	5.1 (0.5)
67.85	880 (60)	189.65	15 (7)
84.68	107 (7)	191.39	260 (20)
100.11	580 (40)	198.34	157 (13)
107.13	55 (4)	203.55	19 (2)
108.58	31 (2)	206.00	20 (2)
110.38	4 (4)	208.26	24 (2)
111.07	8.1 (0.6)	209.40	19 (2)
113.68	189 (12)	214.32	43 (3)
116.23	20 (2)	215.73	30 (2)
130.81	290 (20)	217.55	127 (8)
133.80	93 (6)	221.61	250 (20)
145.43	26 (2)	222.07	330 (30)

Table 8 (Contd.)

147.69	35 (3)	226.19	119 (8)
148.86	68 (5)	229.3	1000 <sup>a)</sup>
149.45	35 (3)	247.46	196 (13)
150.25	20 (2)	256.45	370 (30)
151.15	17 (2)	264.07	139 (9)
152.43	330 (20)	276.31	340 (20)
156.39	280 (20)	281.45	221 (15)
286.56	274 (18)	1257.47	41.4 (1.2)
295.9 (0.2)	8 (3)	1273.75	36.7 (1.7)
299.90 (0.1)	49 (10)	1279.8 (0.3)	2.4 (0.3)
300.36 (0.1)	66 (15)	1289.16	29.4 (0.6)
313.98 (0.1)	31 (2)	1291.8 (0.4)	9.1 (0.9)
323.40 (0.1)	68 (5)	1294.0 (0.3)	62.7 (1.2)
339.06 (0.1)	216 (14)	1330.9 (0.2)	14.6 (1.3)
342.03 (0.1)	41 (3)	1342.72	100 (25)
345.46 (0.1)	19 (2)	1373.80	11.5 (0.4)
351.07 (0.1)	400 (30)	1387.40	10.3 (1.0)
357.0 (0.1)	21 (2)	1410.10	10.8 (0.7)
891.92	1.3 (0.2)	1427.29 (0.15)	381 (7)
927.95 (0.1)	14.4 (1.5)	1439.3 (0.3)	6.2 (0.4)
943.2 (0.3)	8.8 (1.4)	1453.05	1.5 (0.3)
959.74	7.8 (1.5)	1521.3 (0.4)	3.7 (0.4)
1001.68	95.7 (3.4)	1560.4 (0.4)	2.8 (0.3)

Table 8 (Contd.)

1044.43	11.1 (0.4)	1631.4 (0.5)	0.49 (0.09)
1076.21 (0.15)	410 (12)		
1088.5 (0.3)	7.7 (0.8)		
1113.29	183 (4)		
1121.28	855 (25)		
1157.31	48.7 (1.2)		
1158.08			
1180.8 (0.3)	21.5 (1.0)		
1189.04	351 (10)		
1221.42	677 (14)		
1230.97	579 (11)		

a) Unless otherwise indicated, error may be taken as  $\pm 0.05$  keV.

b) Normalized to the 229.3-keV  $\gamma$ -ray. Only  $\gamma$ -ray energies and intensities in the region from 84 keV to 360 keV were measured in this study. Energies and intensities below 84 keV are taken from Ha61, and those above 360 keV are taken from Ga72.

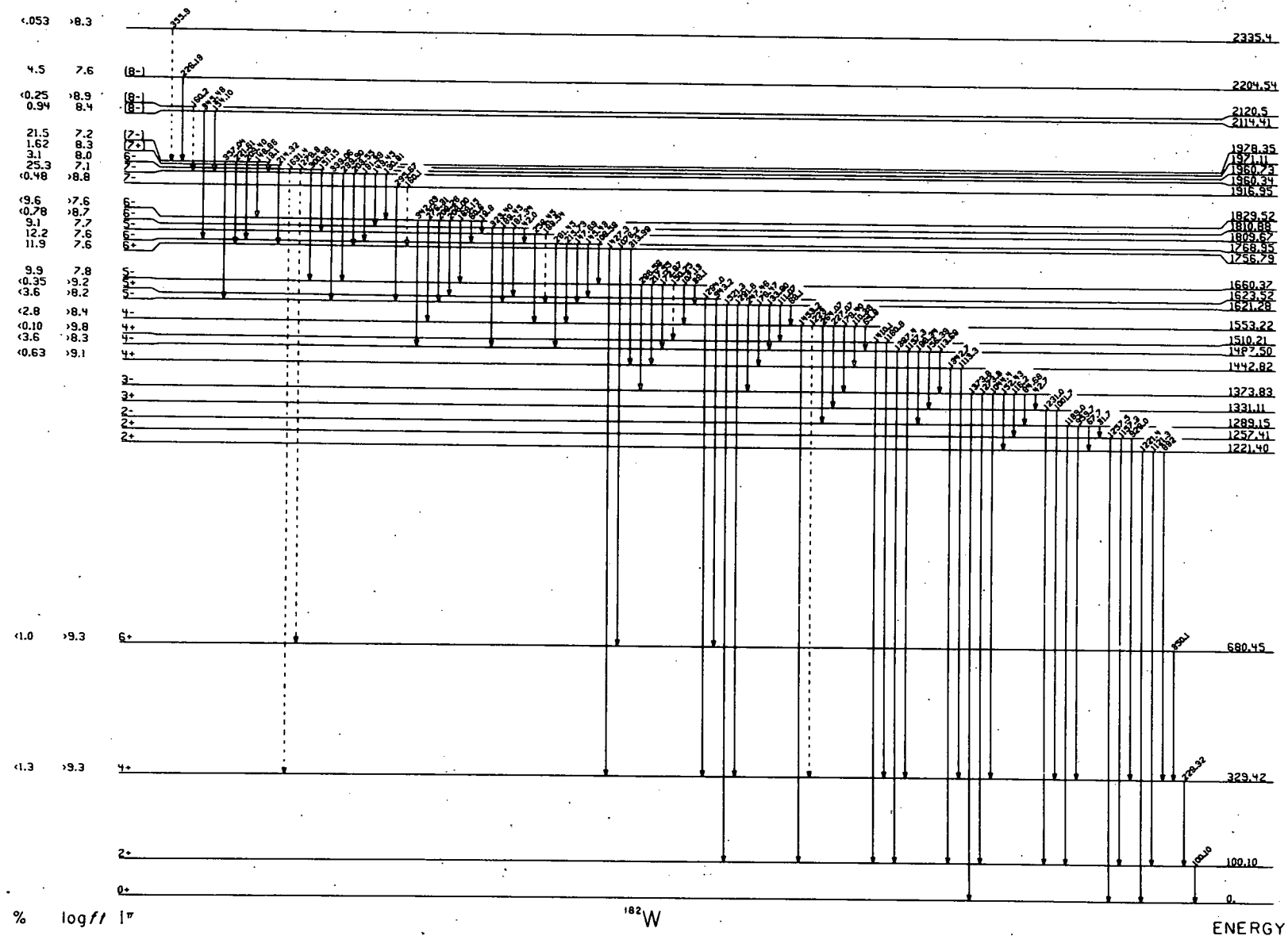


Figure 27. Levels of  $^{182}\text{W}$  populated in the decay of  $64\text{ h }^{182m}\text{Re}$ .

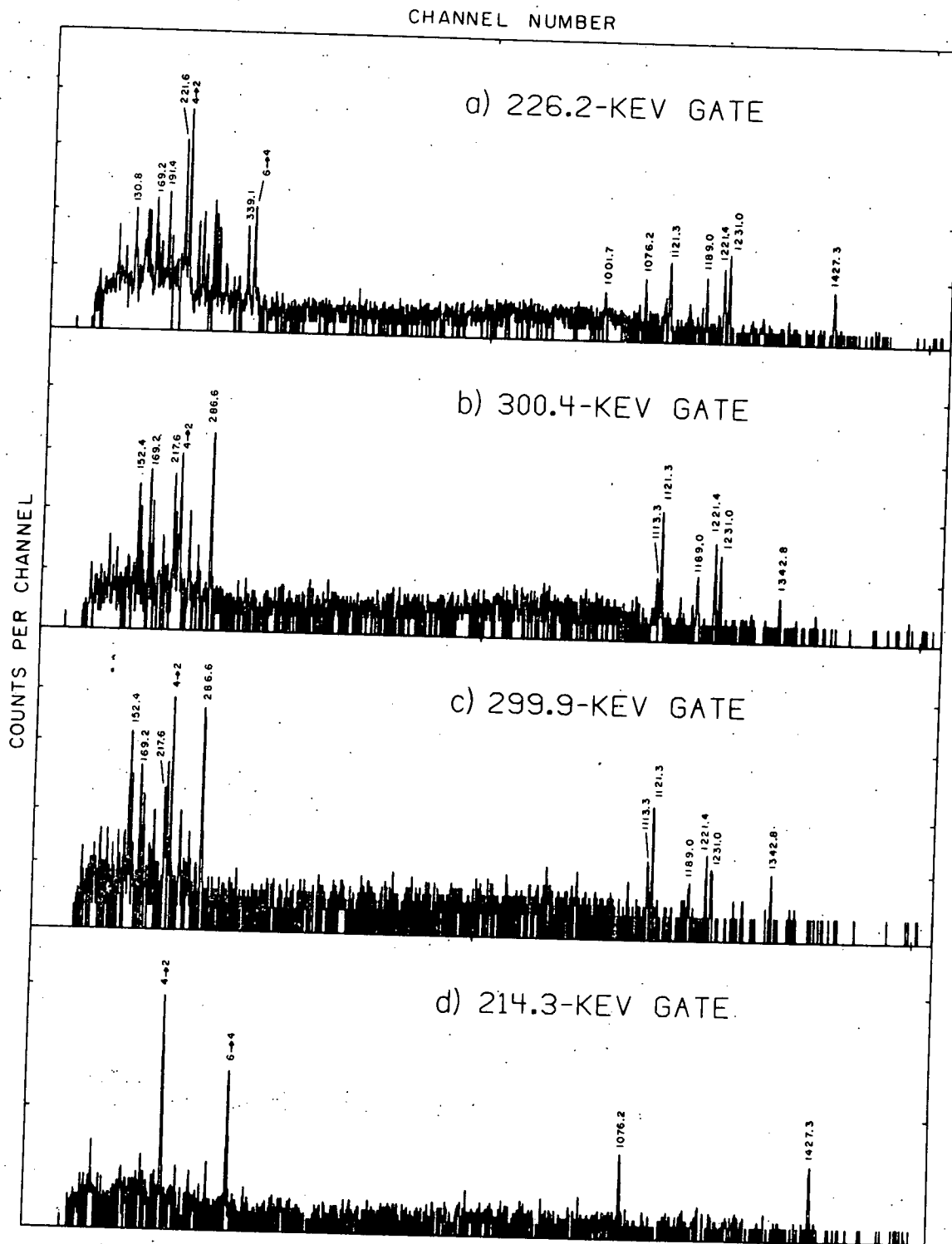


Figure 28. Selected coincidence gates associated with  $^{182m}\text{Re}$  decay.

are proof for the doublet of states at 1960.3 and 1960.7 keV. The 151.2-keV  $\gamma$ -ray could be placed only on the basis of the energy of the transition, and the 131.4-keV transition from the 1960.7-keV state assigned by Harmatz *et al.* [Ha61] was not seen. Figure 28d shows the 214.3-keV gated transition and shows clearly the  $\gamma$ -rays associated with the 1756.8-keV level. The coincidence evidence for the 2335-keV and 2114.4-keV states is weak. However, these levels are firmly established in the in-beam study, so that the decay scheme is believed to be correct.

The intensities of  $\gamma$  rays only in a range from 84 keV to 360 keV were measured in this brief study. The intensities of the higher energy  $\gamma$ -rays were taken from Galan *et al.* [Ga72]. Conversion electron intensities needed to calculate  $\beta$ -decay feedings were obtained when possible from the conversion coefficients quoted by Galan *et al.* [Ga72] or Nilsson *et al.* [Ni67]. In the region below 84 keV, the conversion electron data of Harmatz *et al.* [Ha61] were taken. When no experimental conversion coefficients existed,  $\beta$ -decay feedings were deduced from theoretical conversion coefficient values taken from Hager and Seltzer [HS68] and Dragoun *et al.* [Dr68]. Log<sub>10</sub> values were calculated with use of the tables of Gove and Martin [Go71].

The spin and parity assignments given in the decay scheme are discussed in detail in the previous chapter, though it should be mentioned that the assignment of the  $K^\pi = 6^+$  bandhead at 1756.8 keV as a high-K state (rather than as the spin 6 member of the  $\gamma$  band)

is in agreement with the large  $\text{EC-}\beta^+$  feeding (12%) measured for the state. The information obtained from this decay, especially knowledge of the low energy transitions and  $\text{EC-}\beta^+$  feedings, were invaluable in constructing and interpreting the in-beam level structure, verifying again the theoretical and experimental value of thorough radioactive decay studies.

## **BIBLIOGRAPHY**

## BIBLIOGRAPHY

[Ag70] V. A. Ageev, V. I. Gavrilyuk, T. Kupryashkin, G. D. Latyshev, I. N. Ljutyyj, Yu. V. Makoveckij, and A. I. Feoktistov, *An. SSSR, ser. fiz.*, 34, 2135(1970).

[Al64] P. Alexander, F. Boehm, and E. Kankeleit, *Phys. Rev. B*, 133, 284(1964).

[Ala55] G. Alaga, K. Alder, A. Bohr, and B. R. Mottelson, *K. Danske Vidensk. Selsk. Mat.-fys. Medd.* 29, No. 9 (1955).

[Alc58] D. G. Alchazov *et al.*, *ZhETF (USSR)* 35, 1325(1958); *Izv. Akad. Nauk SSSR (ser. fiz.)* 28, 229(1964).

[Be71] F. M. Bernthal, J. O. Rasmussen, and J. M. Hollander, *Phys. Rev. C* 3, 1294(1971).

[Be74a] F. M. Bernthal, to be published.

[Be74b] F. M. Bernthal, B. D. Jeltema, J. S. Boyno, T. L. Khoo, and R. A. Warner, *Phys. Rev. Lett.* 33, 915 (1974).

[Bel59] S. T. Belyaev, *Mat. Fys. Medd. Dan. Vid. Selsk.*, 31, No. 11(1959).

[Bem73] C. E. Bemis, P. H. Stelson, F. K. McGowan, W. T. Milner, J. L. C. Ford, Jr., R. L. Robinson, and W. Tuttle, *Phys. Rev. C* 8, 1934(1973).

[Dr68] O. Dragoun, H. C. Pauli, and F. Schmutzler, *Max Planck Institute Report No. MPIH-1968-V14*, 1968(unpublished).

[Ga72] P. Galan and M. Vejs, *Czech. J. Phys.* B22, 18(1972).

[Gi67] P. Gilad, G. Goldring, R. Herber, and R. Kalish, *Nucl. Phys.*, A91, 633(1967).

[Go71] N. B. Gove and M. J. Martin, Nucl. Data A10, No. 3 (1971).

[Gü72] C. Günther, P. Kleinheinz, R. F. Casten, and B. Elbeck, Nucl. Phys. A172, 273(1971).

[Ha61] B. Harmatz, T. H. Handley, and J. W. Mihelich, Phys. Rev. 123, 1758(1961).

[Ha67] A. J. Haverfield, F. M. Bernthal, and J. M. Hollander, Nucl. Phys. A94, 337(1967).

[He72] P. Herzog, M. J. Canty, and K. D. Killig, Nucl. Phys. A187, 49(1972).

[He73] D. L. Hendrie, Phys. Rev. Lett. 31, 478(1973).

[Hj68] S. A. Hjorth, H. Ryde, and B. Skånberg, Arkiv för Fysik 38, 537(1968).

[HS68] R. S. Hager and E. C. Seltzer, Nucl. Data A4, Nos. 1 and 2 (1968).

[Hu73] S. Hultberg, I. Rezanka, and H. Ryde, Nucl. Phys. A205, 321(1973).

[Je74] B. D. Jeltema and F. M. Bernthal, Phys. Rev. C 10, 778 (1974).

[Kh73] T. L. Khoo, J. C. Waddington, and M. W. Johns, Can. J. Phys. 51, 2307(1973).

[Kh73b] T. L. Khoo, J. C. Waddington, Z. Preibisz, and M. W. Johns, Nucl. Phys. A202, 289(1973).

[K173] P. Kleinheinz, P. J. Daly, and R. F. Casten, Nucl. Phys. A208, 93(1973).

[Li73] Th. Lindblad, H. Ryde, and P. Kleinheinz, Nucl. Phys. A210, 253(1973).

- [Ma67] E. R. Marshalek, Phys. Rev. 158, 993(1967).
- [Ma74] H. Massmann, J. O. Rasmussen, T. E. Ward, P. E. Haustein, and F. M. Bernthal, Phys. Rev. C 9, 2312(1974).
- [Mo55] S. A. Moszkowski, in Beta- and Gamma-ray Spectroscopy, edited by K. Siegbahn (Interscience Publishers, New York, 1955), Chap. XIII.
- [Na64] O. Nathan and S. G. Nilsson, in Alpha-, Beta-, and Gamma-ray Spectroscopy, edited by K. Siegbahn (North-Holland, Amsterdam, 1964), p. 601.
- [Ne70] K. Neergård and P. Vogel, Nucl. Phys. A145, 33(1970).
- [Ni55] S. G. Nilsson, K. Danske Vidensk. Selsk. mat.-fys. Medd. 29, No. 16 (1955).
- [Ni67] Ö. Nilsson, S. Höglberg, S. E. Karlsson, and G. M. El-Sayad, Nucl. Phys. A100, 351(1967).
- [Ni69] S. G. Nilsson and Chin Fu Tsang, Nucl. Phys. A131, 1(1969).
- [No71] R. Nordhagen, R. M. Diamond, and F. S. Stephens, Nucl. Phys. A138, 231(1971).
- [Ri68] F. A. Rickey, Jr., and R. K. Sheline, Phys. Rev. 170, 1157(1968).
- [Sa70] J. J. Sapyta, E. G. Funk, and J. W. Mihelich, Nucl. Phys. A139, 161(1970).
- [SG65] P. H. Stelson and L. Grodzins, Nucl. Data A1, No. 1 (1965)21.
- [St72] F. S. Stephens and R. S. Simon, Nucl. Phys. A183, 257(1972).
- [St74] F. S. Stephens, P. Kleinheinz, R. K. Sheline, and R. S. Simon, Nucl. Phys. A222, 235(1974).

[Wa73] R. A. Warner, F. M. Bernthal, J. S. Boyno, and T. L. Khoo, Phys. Rev. Lett. 31, (1973) 34.

[We61] H. I. West, Jr., L. G. Mann, and R. J. Nagle, Phys. Rev. 124, 527 (1961).

[Ya68] T. Yamazaki and G. T. Ewan, Nucl. Instr. and Meth. 62, 101 (1968).